Hydrological Sciences Journal

ISSN: 0262-6667 (Print) 2150-3435 (Online) Journal homepage: www.tandfonline.com/journals/thsj20

Separating baseline conditions from anthropogenic impacts: example of the Damour coastal aquifer (Lebanon)

Wisam M. Khadra & Pieter J. Stuyfzand

To cite this article: Wisam M. Khadra & Pieter J. Stuyfzand (2014) Separating baseline conditions from anthropogenic impacts: example of the Damour coastal aquifer (Lebanon), Hydrological Sciences Journal, 59:10, 1872-1893, DOI: 10.1080/02626667.2013.841912

To link to this article: https://doi.org/10.1080/02626667.2013.841912

http://dx.doi.org/10.1080/02626667.2013.841912

Separating baseline conditions from anthropogenic impacts: example of the Damour coastal aquifer (Lebanon)

Wisam M. Khadra[1,2] and Pieter J. Stuyfzand[1,3]

[1]VU University Amsterdam, Critical Zone Hydrology Group, 1081 HV Amsterdam, The Netherlands
w.khadra@vu.nl

[2]Department of Geology, American University of Beirut, 1107 2020 Riad El-Solh, Beirut, Lebanon

[3]KWR Watercycle Research Institute, 3430 BB Nieuwegein, The Netherlands

Received 1 April 2013; accepted 24 July 2013; open for discussion until 1 April 2015

Editor D. Koutsoyiannis; **Associate editor** A. Fiori

Abstract A new structured approach is presented to derive groundwater baseline conditions, in this case for a dolomitic limestone aquifer suffering from salinization and other anthropogenic impacts. It builds on the HydroChemical System Analysis (HCSA) to map different groundwater bodies (hydrosomes) and hydrochemical zones within them, each of which show significant differences in baseline conditions. It also comprises a rigorous elimination scheme for samples affected by bias or pollution. The method is applied to the Damour coastal aquifer system, south of Beirut (Lebanon). Concentrations of Cl, Cl/Br, ^{2}H, ^{18}O and Ca/Sr were used to discern five hydrosomes and to determine mixing ratios. The dominant hydrochemical facies was (sub)oxic, calcareous and salinized, indicating a very low reduction capacity of the aquifer system, strong dissolution of dolomitic limestone and clear traces of seawater encroachment. The method proposed was capable of filtering out baseline conditions for 16 main constituents, 64 trace elements and two isotopes.

Key words baseline chemistry; system analysis; groundwater mapping; multi-tracing; salinization; Lebanon

Séparer conditions originelles et impacts anthropiques: l'exemple de l'aquifère côtier de Damour (Liban)

Résumé Nous présentons une nouvelle approche structurée de détermination des conditions originelles des eaux souterraines, ici pour un aquifère calcaire dolomitique subissant une salinisation et d'autres impacts anthropiques. Il s'appuie sur l'Analyse de Système Hydrochimique pour cartographier différentes structures d'eaux souterraines (hydrosomes) et des zones hydrochimiques en leur sein, chacune d'elles montrant des différences importantes de ses conditions originelles. Il comprend également un système d'élimination rigoureuse des échantillons affectés par des biais ou par la pollution. La méthode a été appliquée au système aquifère côtier de Damour, au sud de Beyrouth (Liban). Cl, Cl/Br, ^{2}H, ^{18}O et Ca/Sr ont été utilisés pour identifier cinq hydrosomes et déterminer des coefficients de mélange. Le faciès hydrochimique dominant est suboxique, calcaire et salé, indiquant une très faible capacité de réduction du système aquifère, une forte dissolution du calcaire dolomitique et des traces évidentes d'intrusion d'eau de mer. La méthode proposée a été capable de retrouver les conditions originelles pour 16 constituants principaux, 64 éléments traces et deux isotopes.

Mots clefs chimie de base ; analyse de système ; cartographie des eaux souterraines ; multi-traçage ; salinisation ; Liban

1 INTRODUCTION

Coastal aquifers are gaining a special interest in hydrogeology due to their hydraulic complexity and overexploitation to supply water to urbanized coastal zones, where more than half of the world's population is living (Essink 2001, Post 2005, Bobba 2007). They are also known for their complex hydrochemical nature due to a wide spectrum of groundwater origins, salinity sources, alkalinity, redox potential, the extent of cation exchange, and anthropogenic causes of contamination (Stuyfzand 1993). In general, the future of coastal aquifers is not so bright, and water-resource managers are under a real challenge to protect their groundwater supplies (Sanford and Pope 2010).

This study focuses on a Mediterranean karstic, coastal aquifer of Cretaceous age, the Damour

aquifer system, south of Beirut (Lebanon). This aquifer was chosen in the late 1970s as an alternative to the capital's main aquifer which was contaminated by seawater intrusion (Khadra 2003). A large amount of groundwater (≈10 hm^3/year) is being extracted from the aquifer, 80% of which feeds part of the capital Beirut and its suburbs (Khadra 2003, CAMP 2004).

Karstified aquifers provide the main source of groundwater in many Mediterranean regions (El-Hakim and Bakalowicz 2007). Their multitude of water quality problems has generated many studies, for instance by Mandel *et al.* (1972), Kafri and Arad (1979), Stigter *et al.* (1998), Tulipano *et al.* (2005), Kempe *et al.* (2006), Abdul Rahman (2007), Weinstein *et al.* (2007), and El-Fiky (2010). Water quality problems also call for an assessment of baseline conditions of such aquifers, for several reasons (Edmunds and Shand 2008): (a) to be able to assess quantitatively whether or not anthropogenic pollution is taking place, (b) to improve groundwater monitoring systems, (c) to breach guidelines for potable water quality when the concentration of certain elements is quite natural, (d) to define zones of uncontaminated water and protect these areas better, and (e) to provide guidelines for new policy, engagement with end users such as water utilities, and the general public. This need is even more acute for coastal karstic aquifers, because of their extreme vulnerability to salinization and other sources of pollution (Tulipano *et al.* 2005).

Hydrochemical studies of the Lebanese groundwaters (Arkadan 1999, Khadra 2003, Saad *et al.* 2004, Korfali and Jurdi 2007, Saadeh 2008, Korfali and Jurdi 2009) did not address their baseline conditions. The term "baseline" is defined in this study as "the range of concentrations of a given element, isotope or chemical compound in solution, derived entirely from natural, geological, biological or atmospheric sources, under conditions not perturbed by anthropogenic activity" (Edmunds and Shand 2008).

To date, the literature summarized by Edmunds and Shand (2008) lacks a standardized comprehensive methodology to establish groundwater baseline chemistry once a monitoring network has been defined and sampled. It covers a backward trend analysis of young groundwaters or, if available, the selection of a data subset from older monitoring networks that is assumed to reflect the natural composition, as evidenced by hydrological and geochemical tracers. However, it does not cover a scheme to fully eliminate data affected by bias or pollution (especially relevant for trace elements), and a method to define groundwater bodies and hydrochemical facies within them, each of which requires its own baseline chemistry. We therefore developed a new approach, consisting of a six-step procedure that incorporates:

1. an elimination scheme for data effected by bias or pollution;
2. the HydroChemical System Analysis (HCSA) as proposed by Stuyfzand (1999, 2005) to distinguish different groundwater bodies (hydrosomes) and hydrochemical zones (facies) within them;
3. historical data evaluation; and
4. statistical analysis.

2 SETTING AND METHODS

2.1 Geological and hydrogeological setting

The 60-km^2 study area belongs to the western flanks of the Lebanese range called the Mediterranean Province (Lebanese Ministry of Environment 2001). It lies along the coastal zone of Lebanon, at about 7 km south of the capital Beirut (Fig. 1). It is characterized by two main topographical features. The first is a flat coastal plain in the west, which slopes very gently seaward, it is known as a cultivation strip. The second is a hilly, sloping terrain reaching a maximum elevation of about 550 m at the eastern boundary. The Damour River is the most important perennial river, whilst most other valleys are less deep and contain ephemeral streams (Fig. 1).

The study area has a humid mesothermal Mediterranean climate characterized by dry summer and relatively mild moist winter with abundant sunshine. The wet season extends from November to April, with sparse precipitation events in May, September and October (Arkadan 2008). The northeast trending Lebanese mountain range acts as a barrier of humid westerly winds enhancing the effect of orographic precipitation to the west. Records between 1985 and 2009 (Meteorological Service 2010) show an annual precipitation of between 352 and 1163 mm, with an arithmetic mean of 770 mm. A climatic cycle is expected at a recurrence interval of 14 years (Arkadan 2008).

Land-use patterns show 12% urbanized zones (including residential houses and transportation facilities), 14% agricultural lands (mainly banana plantations and vegetable gardening), while the remaining 74% form grass, vegetation and bare land cover. This has been the dominant area distribution over the last decades, although minor expansion of urbanization occurred in the mid-1990s, with high development at

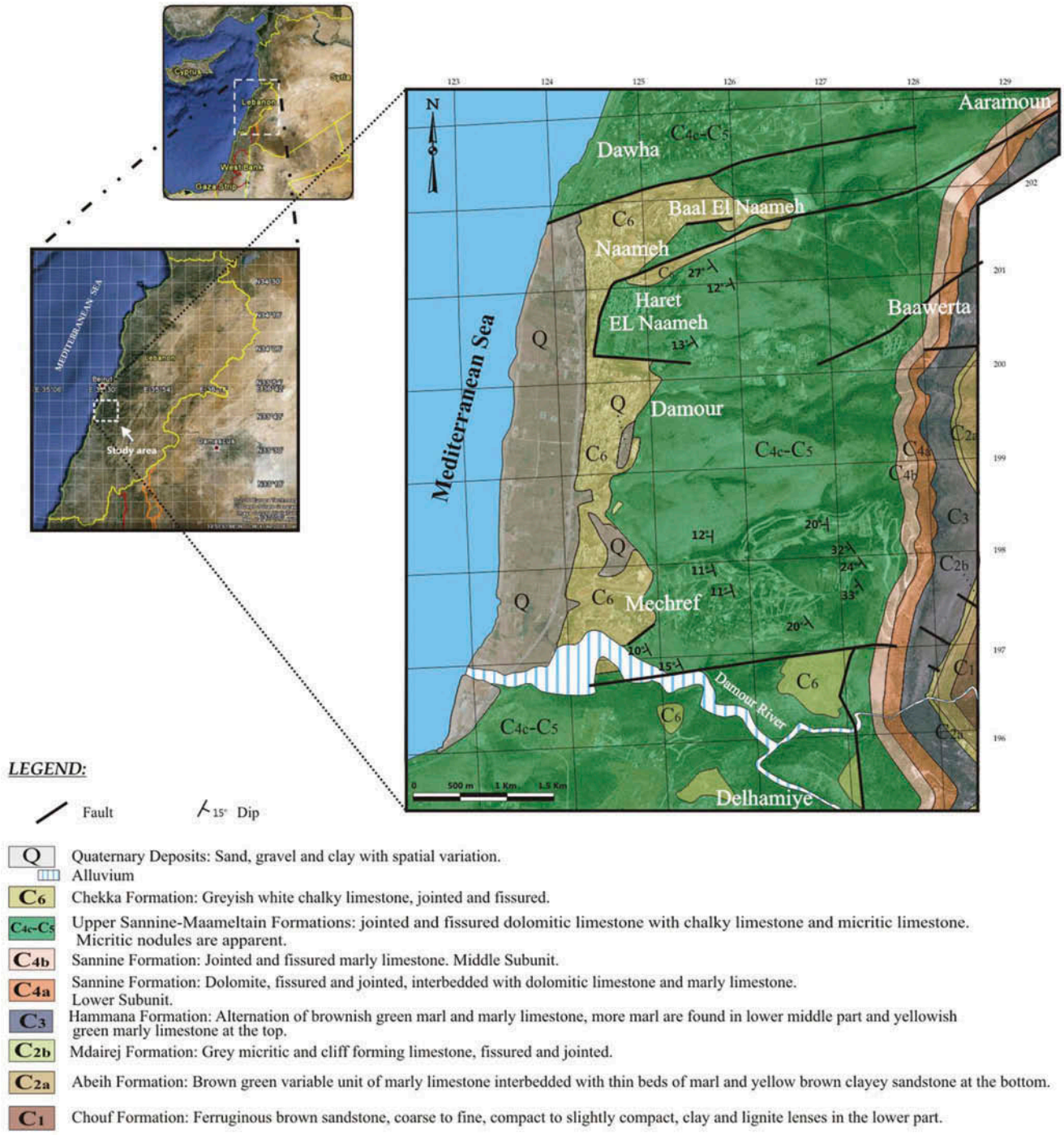

Fig. 1 Geological map of the Damour area (modified after Khadra 2003).

altitude zones exceeding 150 m that were only partially inhabited before (CAMP 2004). Industrial activities are scarce, apart from an important small area in Haret El Naameh village where floor tiles and refrigerators are manufactured.

Rock types are divided into eight main formations following the stratigraphic division in Lebanon. The exposed units range in age from the Cretaceous to recent (Fig. 1). Six major and some minor faults dissect the area. They are sub-parallel and approximately east–west oriented (Khadra 2003). The general dipping of layers is westward, with some deviations due to faulting. The dip reaches its maximum inclination (55°) at the eastern part of the area.

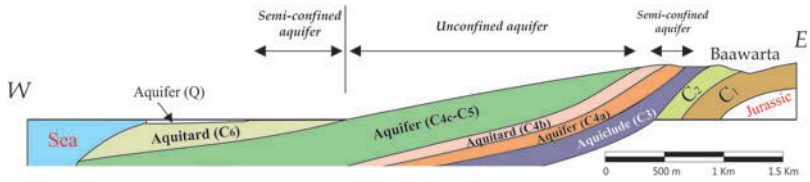

Fig. 2 Hydrogeological cross-section (modified after Khadra 2003). Symbols, as shown in Fig. 1, vertical scale is the same as horizontal.

It decreases in a westward direction, reaching its minimum (8°) at the Maameltain-Chekka Formation boundary (Figs 1 and 2).

The Damour hydrological system (Fig. 2 and Table 1), is made up of a main upper aquifer (C_{4c}–C_5), underlain by a semi-confining unit (C_{4b}) and a relatively thin lower aquifer (C_{4a}). The upper aquifer is covered by a minor small aquifer of very thin Quaternary deposits (Q). We assume that the middle semi-confining unit (C_{4b}) does not hinder the hydraulic connection between the two units whereas the Hammana formation (C_3), dominated by marly layers, forms an impermeable base of the system.

The Damour upper aquifer is only semi-confined in the west, while exposed to the surface in its greater part (Fig. 1); it has few paved surfaces and, hence, is capable of receiving recharge from precipitation across a wide portion of its exposed parts. Recharge, as a percentage of precipitation, was estimated using a water balance approach (Khadra 2003). Neglecting storage changes, the average recharge to the upper aquifer (≈ 35 km^2 exposed in the study area) is estimated at 28% of gross precipitation (Table 2).

Table 2 Water budget components estimated between April 2001 and March 2002 (modified after Khadra 2003).

Component	Value (mm/year)	Value (%)	Area[2] (km^2)	Value (hm^3/year)
Precipitation	825	100	49	40
Evapotranspiration	327	40	49	16
Runoff	261	32	49	13
Recharge	237	28	49	11
Irrigation return flow[1]	900	–	8	7
Pumped volume	–	–	–	10

[1]Estimate based on land use and average weekly irrigation consumption. The Damour River provides a major portion of this water, which is diverted through small canals.
[2]The area excludes residential spots and transportation facilities.

2.2 Data collection

A sampling campaign was launched in 2011/12 to collect 102 samples (Fig. 3) from rainfall, pumping wells, the Damour River and the Mediterranean Sea, in order to build a reliable, homogeneous hydrochemical database covering a wide range of parameters (four physical, 73 chemical, and two isotopic). This dataset was added to the few data previously collected by others since 1979 (Ajam and Saa'd 1980a, 1980b, Dar Al-Handasah 1999, Khadra 2003, Saad *et al.* 2004).

Two raingauges were installed at 1 km and 3.7 km from the shoreline (Fig. 3) to collect rainfall on a daily basis. Cumulative samples were sent to the laboratory for detailed chemical analyses every two weeks. For groundwater, pumping wells were sampled, because dedicated monitoring wells were absent (as in the whole of Lebanon and in many hardrock areas elsewhere). Wells were drilled by either percussion or rotary drill, and had 6- to 40-m-long well screens, or none. Using pumping wells for water quality monitoring introduces specific problems, such as mixing of different water qualities (Mendizabal and Stuyfzand 2009). The recent sampling campaign tried to avoid other

Table 1 Generalized description of the hydrostratigraphic units in the Damour area (from surface to bottom).

Hydrogeological unit	Geological unit	Symbol	Approximate thickness (m)	Description
Minor aquifer	Quaternary	Q	5	Gravel, sand and clay
Aquitard	Chekka	C_6	160	Marly limestone
Aquifer	Upper Sannine-Maameltain	C_{4c}-C_5	400	Dolomitic limestone
Aquitard	Middle Sannine	C_{4b}	70	Marly limestone
Aquifer	Lower Sannine	C_{4a}	80	Dolomite and limestone
Aquiclude	Hammana	C_3	200	Marl and marly limestone

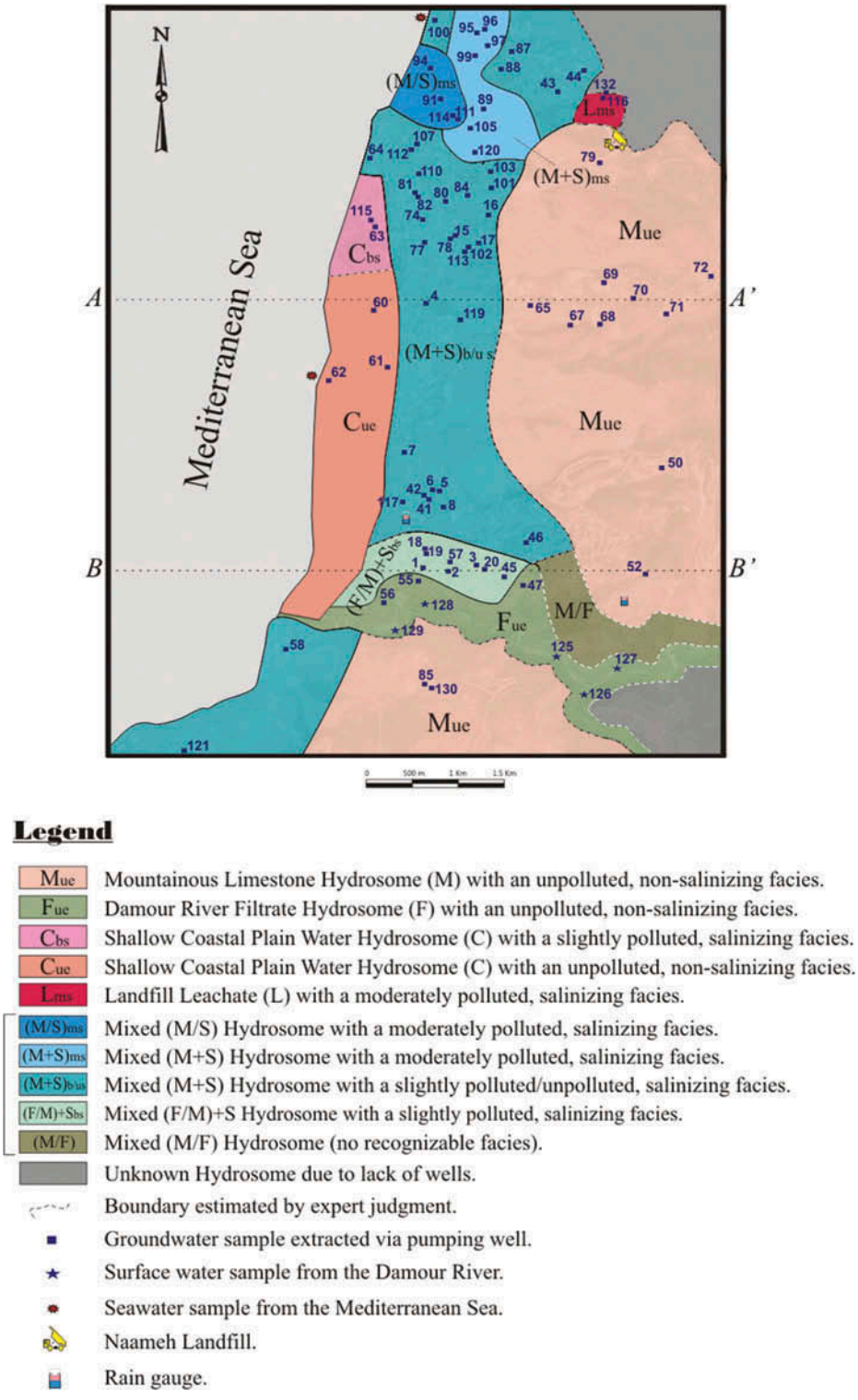

Fig. 3 Hydrochemical map showing the spatial distribution of hydrosomes and their main hydrochemical facies. All mapped hydrosomes are calcareous and (sub)oxic.

problems by pumping the wells for a long time to ensure proper purging, requiring the evacuation of more than three standing volumes and a stable electrical conductivity (EC). Purging was not needed for government wells (20% of all wells), as they are continuously pumping for most of the year, nor for municipal wells (15% of wells) that run for most of the day. Pumping rates were

1000–4000 m^3/d for government wells, 150–650 m^3/d for municipal wells, and 5–20 m^3/d for private wells. Significant inflows of groundwater from shallow perched zones can probably be neglected in most cases, because it is common practice in Lebanon to stop drilling once groundwater appears.

Different sets of bottles were used for separate analyses: high-quality HDPE bottles for metals (100 mL) and for alkalinity, nitrate and ammonium (500 mL). Each bottle was cleaned in the laboratory and rinsed with distilled water, except for the 100-mL bottles that were rinsed in the laboratory 2–3 times with a small volume of 1:1 diluted HNO_3, followed by another rinsing with ultrapure water. The acid-rinsed 100 mL PE bottles (for major and trace elements) were filled after filtration in the field using 0.45-µm syringe filters, and acidified in the laboratory, on the same day, by adding 65% suprapure HNO_3 to pH < 2 (0.7 mL of 65% HNO_3 to 100 mL of water). The 500-mL bottles were cooled to 4–8°C, and the more mineralized samples (EC > 1500 µS/cm), to be analysed by ICP-ES/ICP-MS, were diluted maximum 1:3 before delivery to the laboratory.

Most water samples were analysed for: (a) EC, pH and temperature, *in situ*, with a SevenGo Duo pro water quality meter (Mettler, Toledo), (b) O_2 *in situ*, using a SX726 DO meter (Sanxin), (c) alkalinity by titration (HACH 8221), NO_3 by spectrophotometry (HACH 8039) and NH_4 by spectrophotometry (APHA 4500-C), in the American University of Beirut Core Lab, (d) main cations, Cl, Br, SO_4, Si, P and 62 trace elements (including heavy metals, rare earth elements and others), by ICP-ES/ICP-MS in AcmeLabs Vancouver, and (e) ^{18}O and ^{2}H by pyrolysis and mass spectrometry in the isotope laboratory of VU University Amsterdam.

The trace elements were analysed with a detection limit of 0.01–0.05 µg/L. Isotopes are reported as δ notation in per mil relative to Vienna-Standard Mean Ocean Water ($‰_{V\text{-}SMOW}$).

Duplicates, blanks and spikes showed acceptable results. Additional checks of the accuracy of the chemical analyses showed excellent ionic balances and measured ECs that closely matched the ECs calculated with Hydrogeochemcal (HGC 2.1, Stuyfzand 2012). Bird dropping correction was also applied to precipitation where necessary. This is a correction procedure to biogenic contributions from bird droppings, insect droppings, plant and animals debris, etc.

2.3 HydroChemical System Analysis

The HydroChemical System Analysis (HCSA; Stuyfzand 1999, 2005) is composed of a three-step approach starting with discriminating different water bodies of different origin (hydrosomes), then stepping down by characterizing hydrochemical zones (hydrochemical facies) within each hydrosome, and finally, if needed, identifying chemical water types. In this study, a hydrochemical map was constructed displaying the spatial distribution of hydrosomes and hydrochemical facies within them, and, in a next step, the baseline hydrochemistry for the different units was assigned.

2.3.1 Identification of hydrosomes via environmental tracers A hydrosome is a coherent 3D groundwater body with a specific origin. Hydrosomes can be identified and their boundaries established by combining information on geomorphology, groundwater flow, geophysics, hydrogeological structure, and water quality. The latter includes environmental tracers, which indicate the source water and water–rock interactions. Good tracers are couples such as δ^2H–$\delta^{18}O$ (Bouchaou *et al.* 2008), $\delta^{18}O$–Cl (Stuyfzand 1993), Cl–Br (Stuyfzand 1993, Alcalá and Custodio 2004, Cartwright *et al.* 2006, de Montety *et al.* 2008), Cl-SO_4 (Petelet-Giraud *et al.* 2007), Cl–HCO_3 (Lee and Song 2007) and Ca–Sr (Brenot *et al.* 2008), preferably in combination with major ions and less immobile trace elements such as B and Li to provide a full hydrochemical fingerprint.

2.3.2 Determination of hydrochemical facies Hydrosomes can be subdivided into several characteristic zones, called hydrochemical facies, based on boundaries in chemical composition. Compositional variations are expected to occur along flow lines even within a single facies (Camp and Walraevens 2008). They are due to changes in recharge composition, flow patterns and the chemical interaction between the water and surrounding medium (Stuyfzand 1993, 1999).

The hydrochemical facies is determined by combining four indices regarding redox state, water pollution, mineral saturation (normally calcite) and base exchange. These facies parameters and their codes are summarized in Table 3. The four indices were determined from the available water quality analyses, using Hydrogeochemcal (HGC 2.1, Stuyfzand 2012). Most samples (95%) clearly showed interaction with dolomitic limestone ($Ca_{0.7}Mg_{0.3}(CO_3)_2$), the

Table 3 Hydrochemical facies parameters (after Stuyfzand 2005).

Code	Facies parameter pH classes	Description/Criterion
c	calcareous	pH > 6.2
a	slightly acidic	5.0 < pH < 6.2
A	acid	pH < 5.0
	Redox index[1]	Based on the major redox sensitive species in water (O_2, NO_3, SO_4, Fe-total, Mn-total, NH_4 and CH_4)
o	(sub)oxic	0–2
r	reduced (anoxic)	3–4
d	deeply anoxic	5–6
x	mixed	
	Pollution index (WAPI)*[1]	*
u	unpolluted	0–2
b	slightly polluted	2–6
m	moderately polluted	6–20
p	polluted	>20
	Base exchange index (BEX)	$BEX^2 = Na^+ + K^- + Mg^{2+} - 1.0716\ Cl^-$ $BEX^3 = Na^+ + K^- - 0.8768\ Cl^-$
e	equilibrium	0 (zero)/no BEX (e)
f	freshened	> +(0.5 + 0.02 Cl)/positive BEX (+)
s	salinized	< –(0.5 + 0.02 Cl)/negative BEX (–)

[1]Redox index and WAPI are calculated following rigorous criteria explained in detail in Stuyfzand 2012.
* WAPI is determined on the basis of maximum 10 quality indices (Stuyfzand 2012): aesthetics, acidity#, oxidation/reduction capacity#, nutrients#, total salt content#, organic and inorganic micropollutants#, pesticides, radioactivity and microbiology. The available data in this study allowed WAPI to be based on the five indices labelled with #.
[2]After Stuyfzand (1986), for aquifers without dolomite.
[3]After Stuyfzand (2008), for aquifers containing dolomite or dolomitic limestone.

Table 4 Spectrum of chemical water type parameters observed in the study area, combining into a code like F4CaHCO$_3$+.

Code	Parameter Chlorinity (main type)	Description/Criterion Chloride concentration in sampled water (mg/L)
g	Oligohaline-fresh	5–30
F	Fresh	30–150
f	Fresh-brackish	150–300
B	Brackish	300–1000
b	Brackish-salt	1000–10 000
S	Salt	10 000–20 000
H	Hypersaline	>20 000
	Alkalinity (type)	Alkalinity as HCO_3 (mg/L)
*	Very low	<31
0	Low	31–61
1	Moderately low	61–122
2	Moderate	122–244
3	Moderately high	244–488
4	High	488–976
	Dominant cation and anion (subtype)	Most important cation and anion
Ca	Calcium	The strongest family members discovered to date are placed in the appropriate fields inside two triangles constructed for this purpose (Stuyfzand 1989)
Mg	Magnesium	
Na	Sodium	
HCO_3	Bicarbonate	
Cl	Chloride	
Mix	No anion family > 50% of anions sum	
	Base exchange index (BEX); (freshening/ salinizing tendency)	Explained in Table 3
o	No base exchange	Marine cation equilibrium
+	Freshened	Marine cations surplus
–	Salinized	Marine cations deficit

composition of which was derived from their average Ca/Mg ratio corrected for seawater contribution (see Section 2.3.4). This justifies the use of the calcite saturation index in which, however, the log (solubility product) was raised by 0.3 to account for Mg solid solution (Morse and Mackenzie 1990). The omnipresence of dolomitic limestone also necessitated the use of the base exchange index (BEX) without including Mg (Table 3).

2.3.3 Determination of chemical water type The chemical water type is determined following the scheme of Stuyfzand (1989). This method combines in one code consecutively the chlorinity, the alkalinity, the dominating member of the strongest pair of cations and anions within a geohydrochemical family, and the BEX (set in dolomitic limestone mode), which can indicate freshwater or salt-water intrusion (Table 3). As an example, water type F4CaHCO$_3$+ means fresh, high alkalinity, freshened calcium bicarbonate water. The spectrum of water type parameters observed in the study area is shown in Table 4.

2.3.4 Determination of mixing ratios The mixing ratio in a water sample from different hydrosomes needs to be determined for: (a) mapping purposes, (b) identifying geochemical processes and likely source(s) of pollution, including salinization, and (c) calculating the chemical composition of one of the end-members when the composition of the other end-member(s) and the mixing ratio are known. The latter is useful to correct concentrations for seawater admixing.

In our case, the most likely two or three end members to mix in the sampled pumping wells are infiltrated local rain water (either in mountains or in coastal plain), infiltrated Damour River water, and/or intruded Mediterranean Sea water. The solution for two end-members, for instance freshwater and salt water, with a single tracer such as Cl is:

$$\mathrm{Cl_{MIX}} = (1 - f_S)\mathrm{Cl}_F + f_S\mathrm{Cl}_S \quad (1)$$

$$f_S = (\mathrm{Cl_{MIX}} - \mathrm{Cl}_F)/(\mathrm{Cl}_S - \mathrm{Cl}_F) \quad (2)$$

in which: $\mathrm{Cl_{MIX}}$, Cl_F and Cl_S are chloride concentration in mixture, freshwater and saline water, respectively (mg/L), and f_S is the fraction of salt water (-).

By correcting for seawater admixing, any concentration of the freshwater end member (C_{FC}) becomes:

$$C_{\mathrm{FC}} = (C_{\mathrm{MIX}} - f_S C_S)/(1 - f_S) \quad (3)$$

where C_{FC} is the concentration of freshwater end member (mg/L), C_{MIX} is the concentration in mixture (mg/L), C_S is the concentration in saline water (mg/L), and fs is calculated using Cl according to equation (2).

For a mixture composed of three end-members, we need two independent tracers, for instance Cl and ^{18}O, according to the following formulas (modified after Stuyfzand and Stuurman 2006):

$$c = \frac{\left(\delta^{18}\mathrm{O}_R - \delta^{18}\mathrm{O}_L\right)\left(\mathrm{Cl_{MIX}} - \mathrm{Cl}_L\right) + \left(\mathrm{Cl}_R - \mathrm{Cl}_L\right)\left(\delta^{18}\mathrm{O}_L - \delta^{18}\mathrm{O_{MIX}}\right)}{\left(\delta^{18}\mathrm{O}_R - \delta^{18}\mathrm{O}_L\right)\left(\mathrm{Cl}_O - \mathrm{Cl}_L\right)\left(\delta^{18}\mathrm{O_L} - \delta^{18}\mathrm{O}_O\right)\left(\mathrm{Cl}_R - \mathrm{Cl}_L\right)} \quad (4)$$

$$b = \frac{\left(\delta^{18}\mathrm{O_{MIX}} - \delta^{18}\mathrm{O}_L\right) + c\left(\delta^{18}\mathrm{O}_L - \delta^{18}\mathrm{O}_O\right)}{\delta^{18}\mathrm{O}_R - \delta^{18}\mathrm{O}_L} \quad (5)$$

$$a = 1 - b - c \quad (6)$$

where *a, b, c* are fractions of infiltrated ocean, river- and local rain water, respectively, in mixture (-); subscripts *O, R, L*, MIX are the component in groundwater deriving from ocean, river, local rain and the sampled mixture, respectively; Cl is chloride concentration (mg/L), δ^{18}O is ^{18}O content expressed as relative deviation from Standard Mean Ocean Water (‰ SMOW).

In the above approach, conservative behaviour is assumed during mixing and the quality of all end members should be well known. As pointed out by Mendizabal *et al.* (2010), the simultaneous use of various tracers helps to reduce uncertainties in the calculated mixing ratio and in the assumed end-member compositions. Equation (3) can also be used to trace recharge zones prior to salinization once salinized and/or contaminated zones are discerned.

2.4 Determination of groundwater baseline composition

A new comprehensive approach to establish groundwater baseline composition in six steps is presented in Fig. 4 and described below:

1. Eliminate samples with a bad Ionic Balance (IB < 4 if ΣC + ΣA > 8 meq/L, IB < 6 if ΣC + ΣA = 2–8 meq/L, and IB < 10 if ΣC + ΣA < 2 meq/L, where: IB = 100 (ΣC – ΣA)/(ΣC + ΣA) with ΣC, ΣA = sum of cation and anions, respectively), and discard trace element data if affected by either filtration bias (raised Al ≥ 20 µg/L as indicator of suspended clay at 5.5 < pH < 8.5, Stuyfzand 1987), or well corrosion inputs (high Ni + Mo + (V,Cr) from stainless steel or high Cu from copper or brass well screens (raised if Ni > 50 µg/L, Mo > 10 µg/L, V or Cr > 5 µg/L and pH > 6.2, raised if Cu > 50 µg/L at pH > 6.2).
2. Apply HCSA to discern hydrosomes and hydrochemical facies, each of which requiring the determination of its Natural Background Composition (NBC). HCSA also helps to exclude those samples which show mixing of hydrosomes, a mixed redox or a specific pollution level (WAPI > 2). Knowing the sample's position in the normal downgradient hydrochemical evolution and the geochemistry of the aquifer system (dolomitic limestone in our case), assists in detecting anthropogenic anomalies and in selecting the right mineral saturation index on which pH corrections may be based in Step 6.
3. Use NO_3, Cl/Br, Cl, TOC (or COD) as more specific chemical indicators of pollution (NO_3 > 13 mg/L, Cl/Br depends on type of influence

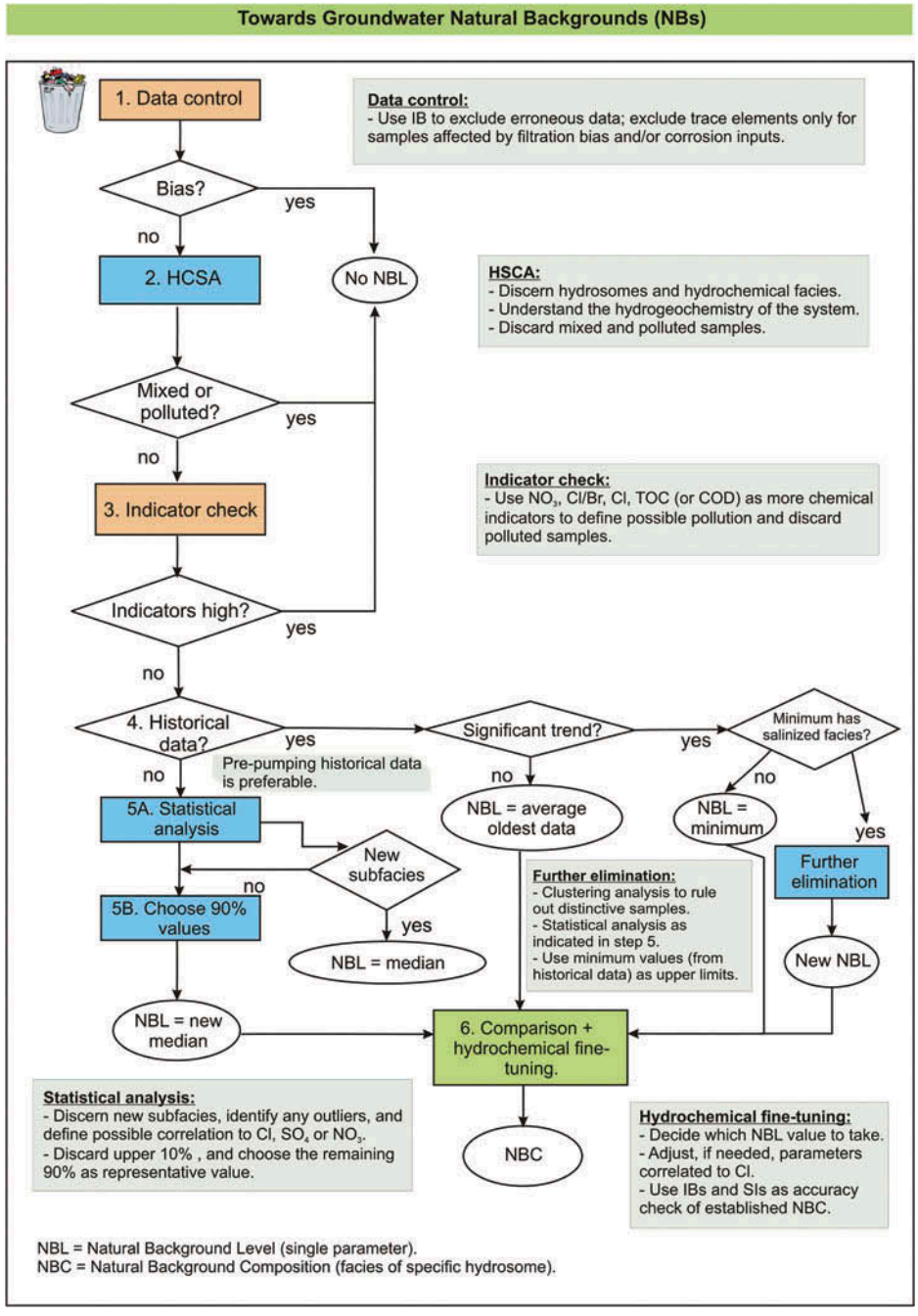

Fig. 4 Flow chart of the new approach proposed for natural background (NB) determination.

(e.g. 500–600 in domestic sewage, see Alcala and Custodio 2004), Cl > 250 mg/L, and TOC > 1.4 mg/L), in addition to WAPI, and discard polluted samples from the "natural background" population.

4. Refer to historical data to define significant hydrochemical trends. In case a significant trend existed for the sampled location, then Natural Backgrounds Levels (NBLs) are the minimum values, otherwise take the average of oldest data as representative of NBLs. Data extending to pre-pumping periods is preferable, although data prior to excessive pumping might suffice. In some cases, notably when minimum values refer to a salinized facies, some further elimination might be required. Expert judgment remains needed to decide whether natural shifts in background quality are taking place, such as in the case of: (i) the natural leaching of soil organic material which leads to a lowering of for instance

Fe(II) and NH_4 base line levels, (ii) natural shifts in coastline position due to sea level fluctuations with an impact on baseline levels for atmospheric Cl, Na and Mg, and (iii) natural vegetation succession which impacts on the evapo-concentration factor F (see equation (7)). This judgement cannot be easily included in any algorithm, but it should make part of Step 4.

5. (a) Do statistical analyses (e.g. correlation matrix, cluster analysis, frequency distribution) to answer three main questions: (i) are there other sample clusters within the facies discerned, indicating a subfacies for which a separate "Natural Background Composition" (NBC) is needed? (ii) are there any outliers as indicated by the frequency distribution? (iii) are there any good correlations with Cl or SO_4 or NO_3 which can help to trim down the NBC in the next step (Step 6)? The latter is useful when there is any correlation between Cl, SO_4 or NO_3 (as pollution indicators) and other parameters. In that case, finding the natural background of one of them (e.g. Na) would benefit from the Na–Cl relationship in extrapolating via the Cl background value.
   (b) Discard the upper 10% of the frequency distribution by taking values below the 90th percentile as representative. Note that these percentages are a matter of dispute and hence other values could be also justified (Edmunds and Shand 2008). For some parameters, notably those mobilized in (deeply) anoxic environments such as Fe, Mn, NH_4 and CH_4, the higher values could better represent the NBLs if their concentration decreased in response to an anthropogenic NO_3 intrusion or a lowering of groundwater tables by pumping.
6. After getting an impression of NBLs via data without and with trend, three final actions are needed: (a) deciding which NBL value to take, (b) checking whether those parameters that strongly correlate with Cl need to be adjusted, and (c) gluing together all NBLs into an NBC for facies X of hydrosome Y. This gluing together requires an accuracy check to ensure that the resulting composition (NBC) shows a correct IB and a pH in accordance with the dominant mineral saturation index (SI_{MIN}) for the aquifer system. If not, then estimate the major constituents with least confidence via IB, and adjust the pH so as to obtain the right SI_{MIN}.

3 RESULTS

3.1 Identified hydrosomes and their facies

The following hydrosomes were identified using multi-tracing: mountainous limestone water (M), Damour River bank filtrate (F), coastal plain water (C), landfill leachate (L), and intruded Mediterranean seawater (S). Relatively pure intruded seawater (presumably >65% current Mediterranean seawater) has not been observed because of mixing with fresh groundwater. This seawater is suspected to occur in the deeper parts of Naameh and Damour coastal strip close to the shoreline. In addition, the mixing ratios for two and three end members aided in further identification of three mixed hydrosomes: M+S, M/S and (F/M)+S. The coding of the mapped hydrosomes and their origins and recharge mechanisms are listed in Table 5. Median values of major constituents are shown in Table 6.

All samples are calcareous and 95% is (sub)oxic. They are close to dolomitic calcite saturation and contain relatively high concentrations of oxidants (O_2, NO_3, SO_4) and very low concentrations of reductants (Fe, Mn, NH_4). Only 5% of all samples showed a mixed redox index due to the coexistence

Table 5 The hydrosomes identified in the study area.

Code	Name	Origin	Main recharge mechanism	% End member
M	Mountainous limestone	Local meteoric	Local precipitation	> 99.9%
F	Damour River bank filtrate	Local meteoric	Remote precipitation, pumping	> 67%
C	Coastal plain water	Local meteoric	Local precipitation	> 99.9%
L	Landfill leachate	Leachate, local meteoric	Local precipitation	–
S	Intruded Mediterranean seawater	Seawater	Pumping	> 67%
M/S	Mixed M/S	Mixture	Precipitation, pumping	10% < S < 67%
M+S	Mixed M+S	Mixture	Precipitation, pumping	0.1% < S < 10%
(F/M)+S	Mixed (F/M)+S	Mixture	Precipitation, pumping	33% < F < 67% & 33% < M < 67%

Table 6 Median composition of groundwater in the study area, grouped on the basis of hydrosomes and hydrochemical facies. Mediterranean seawater, flux weighted average composition of bulk precipitation, and established baseline chemistry for the three major hydrosomes are also shown.

	No. of samples	HCSA code	Chemical water type	EC 25°C (μS/cm)	Temp. (°C)	pH (–)	Cl^-	SO_4^{2-}	HCO_3^-	NO_3^-	P	Na^+	K^+	Ca^{2+}	Mg^{2+}	Fe	Mn	NH_4^+	SiO_2	O_2	δ^2H	$\delta^{18}O$
							(mg/L)														(‰)	
Detection limit							1	1	1	1	0.02	0.05	0.05	0.05	0.05	0.01	5×10^{-5}	0.1	0.04	0.01		
Mountainous limestone (M)	12	M_{coue}	g3CaHCO3o	539	20.2	7.13	27.4	16.5	337	2.0	0.103	11.7	1.5	80.50	29.9	<0.01	0.001	<0.1	11.8	4.7	–26.36	–5.84
Damour river bank filtrate (F)	3	F_{coue}	F2CaHCO3o	515	19.4	7.18	30.2	44.9	250	6.1	0.095	15.4	2.3	78.88	10.5	<0.01	0.000	<0.1	8.1	6.5	–29.25	–6.44
Coastal plain water (C)	5		F3CaHCO3+	803	22.1	6.89	86.2	92.9	328	7.0	0.089	57.7	3.5	119.36	15.3	<0.01	0.001	<0.1	37.2	4.5	–25.06	–5.53
	3	C_{couf}	F3CaHCO3+	759	22.1	6.94	85.1	71.9	312	7.0	0.089	37.7	3.8	115.39	12.7	<0.01	0.001	<0.1	21.5	3.7	–25.63	–5.53
	2	C_{cobs}	f3CaMix–	1094	22.0	6.75	177.0	100.4	336	6.4	0.375	66.5	2.4	187.00	15.9	<0.01	0.001	<0.1	38.4	4.7	–24.71	–5.43
Landfill leachate (L)	1	L_{coms}	b3NaCl–	3947	18.2	6.58	1293.0	206.7	275	3.9	0.220	580.2	18.4	161.37	122.1	0.075	0.001	<0.1	11.4	6.3	–23.81	–5.42
Mixed M/S	4	$(M/S)_{coms}$	b3NaCl–	4561	21.9	7.05	1412.0	209.7	305	6.4	0.318	640.5	28.5	160.65	131.6	0.018	0.002	<0.1	15.3	4.5	–22.10	–4.95
Mixed M+S	70		B3CaCl–	1069	21.0	7.14	240.0	49.4	285	8.9	0.110	86.9	4.7	113.82	42.6	<0.01	0.001	<0.1	11.7	4.4	–24.30	–5.43
	12	$(M+S)_{cous}$	F3CaHCO3–	802	20.9	7.20	141.9	19.9	255	11.3	0.089	31.5	2.9	112.50	34.8	0.213	0.005	<0.1	36.5	3.8	–25.55	–5.57
	58	$(M+S)_{com/bs}$	B3CaCl–	1452	21.2	7.10	359.0	61.5	290	9.0	0.118	147.3	5.6	119.80	45.7	<0.01	0.001	<0.1	11.7	4.4	–24.28	–5.41
Mixed (F/M)+S	15		F3CaMix–	760	18.7	7.20	140.0	36.0	257	5.6	0.095	40.2	2.4	86.29	28.4	<0.01	0.001	<0.1	9.0	3.9	–28.89	–6.29
	9	$(F/M)+S_{cous}$	F2CaHCO3–	691	18.4	7.30	120.0	8.6	240	4.6	0.095	22.5	2.0	76.00	26.0	<0.01	0.007	<0.1	8.6	3.9	–29.04	–6.30
	6	$(F/M)+S_{cobs}$	B3CaCl–	1359	18.7	7.16	308.3	80.1	259	6.2	0.101	141.5	5.6	92.94	39.8	<0.01	0.000	<0.1	9.1	4.6	–28.67	–6.27
Mediterranean Sea	2		H2NaCl	45600	–	7.93	20400	3200	165	4.0	0.510	11600	470	460	1300	0.13	0.002	–	0.06	5.0	7.61	0.95
Precipitation	22		g*CaMix	99	–	7.14	11.2	8.1	24	10.0	0.100	4.9	0.2	8.00	0.7	<0.01	0.003	–	0.3	–	–	–
Established natural backgrounds (NBs)																						
Mountainous limestone (M)		M_{coue}	g3CaHCO3o	519	–	7.20	24.1	12.0	337	1.2	0.100	11.2	1.3	64.0	28.1	<0.01	0.001	<0.1	11.8	4.7	–26.36	–5.95
Damour river bank filtrate (F)		F_{coue}	F2CaHCO3o	505	–	7.29	30.2	43.4	239	5.7	0.086	15.4	2.0	75.1	10.5	<0.01	0.000	<0.1	8.1	5.5	–29.25	–6.44
Coastal plain water (C)		C_{couf}	F3CaHCO3+	757	–	7.05	82.1	71.9	292	5.5	0.084	37.7	2.4	97.1	12.7	<0.01	0.000	<0.1	28.5	3.6	–25.35	–5.53

(*Continued*)

Table 6 (Continued)

	HCSA code	Al	As	B	Ba	Br	Cr	Cu	Ge	La	Li	Mo	Ni	Pb	Pd	Rb	Sb	Sc	Sr	U	V	Zn
		(μg/L)																				
Detection limit		1	0.5	5	0.05	5	0.5	0.1	0.05	0.01	0.1	0.1	0.2	0.1	0.2	0.01	0.05	1	0.01	0.02	0.2	0.5
Mountainous limestone (M)	M_{coue}	2	<0.5	30	9.5	100	0.6	0.9	<0.05	<0.01	1.5	0.3	0.3	0.3	<0.2	0.6	<0.05	1.0	107	0.57	1.2	7.6
Damour river bank filtrate (F)	F_{coue}	1	<0.5	27	34.7	120	0.7	0.7	<0.05	<0.01	2.0	0.3	0.3	0.3	<0.2	0.6	<0.05	<1	136	0.50	0.3	3.8
Coastal plain water (C)		5	1.3	104	82.0	1255	0.9	3.1	0.200	0.01	2.3	3.4	3.1	0.3	<0.2	1.9	0.2	2.8	459	1.98	1.5	96.0
	C_{couf}	3	1.5	50	54.2	382	0.7	1.1	0.120	<0.01	1.5	2.6	4.6	0.3	<0.2	2.1	0.14	2.0	510	1.75	1.5	173.2
	C_{cobs}	3	1.1	161	110.2	1996	1.2	6.1	<0.05	0.023	1.8	0.4	2.4	0.4	<0.2	1.0	0.15	3.5	379	2.71	2.0	37.5
Landfill leachate (L)	L_{coms}	12	3.1	372	27.0	5255	0.6	4.4	0.100	0.15	8.7	0.5	0.3	1.9	0.3	4.6	0.3	1.5	590	0.62	4.5	1159.6
Mixed M/S	$(M/S)_{coms}$	3	5.8	551	135.0	6203	1.0	5.6	0.100	0.03	13.7	3.0	4.4	0.4	0.4	10.3	0.4	1.9	1203	2.14	6.0	413.6
Mixed M+S		2	1.4	156	41.7	1572	0.8	2.1	0.050	<0.01	3.7	0.4	0.7	0.3	0.2	1.9	0.09	1.0	277	0.75	2.4	14.6
	$(M+S)_{cous}$	1	0.8	63	79.4	494	0.5	0.8	0.120	<0.01	2.6	6.2	1.3	0.2	<0.2	1.8	0.06	4.0	641	1.51	0.6	13.0
	$(M+S)_{com/bs}$	2	1.4	160	40.8	1690	0.9	2.1	0.050	0.010	3.8	0.4	0.7	0.3	0.2	2.0	0.10	1.0	276	0.74	2.7	16.0
Mixed (F/M)+S		2	0.9	74	30.6	1110	0.9	1.1	<0.05	<0.01	3.2	0.3	0.1	0.3	<0.2	1.6	<0.05	<1	206	0.56	1.8	3.5
	$(F/M)+S_{cous}$	3	<0.5	35	20.8	348	1.0	1.1	<0.05	<0.01	1.8	0.4	0.5	0.4	<0.2	0.9	<0.05	<1	133	0.51	1.3	3.1
	$(F/M)+S_{cobs}$	2	1.0	92	34.8	1132	0.8	1.2	<0.05	<0.01	3.3	0.3	0.2	0.3	<0.2	1.6	0.05	<1	213	0.56	2.0	6.1
Mediterranean Sea		21	61.6	3750	7.5	82200	5.2	12.5	0.25	0.07	143.0	10.6	3.9	0.5	1.0	125.0	0.22	5.0	7200	2.55	72.0	18.5
Precipitation		8	<0.5	6	5.4	35	0.7	6.1	<0.05	0.01	0.1	0.2	0.7	0.9	<0.2	0.3	0.35	<1	15	0.02	0.4	7.2
Established natural backgrounds (NBs)																						
Mountainous limestone (M)	M_{coue}	2	<0.5	30	8.4	83	0.6	0.9	<0.05	<0.01	0.7	0.2	0.3	0.3	0.100	0.5	<0.05	1.00	78	0.50	1.2	4.1
Damour river bank filtrate (F)	F_{coue}	2	<0.5	27	23.6	120	0.7	0.7	<0.05	<0.01	2.0	0.4	0.3	0.2	0.100	0.6	<0.05	<1	136	0.50	0.3	3.2
Coastal plain water (C)	C_{couf}	2	<0.5	42	51.1	254	0.6	0.9	<0.05	<0.01	1.1	0.2	0.2	0.3	0.100	1.0	<0.05	2.00	236	0.84	0.3	3.3

For all hydrosomes:
Ce, Cs, Dy, Er, Eu, Gd, Ho, In, Lu, Nb, Nd, Pr, Pt, Re, Rh, Tb, Tl, Tm, Y, Yb, < 0.01 μg/L.
Co, Hf, Sm, T, Zr, < 0.02 μg/L, Ag, Au, Be, Bi, Cd, Ga, Ru, Sn, Te, Th, < 0.05 μg/L.
Hg < 0.1 μg/L, Th, Tl, Tm, Y, Yb.
Zr < 0.5 μg/L.
Ti < 10 μg/L.

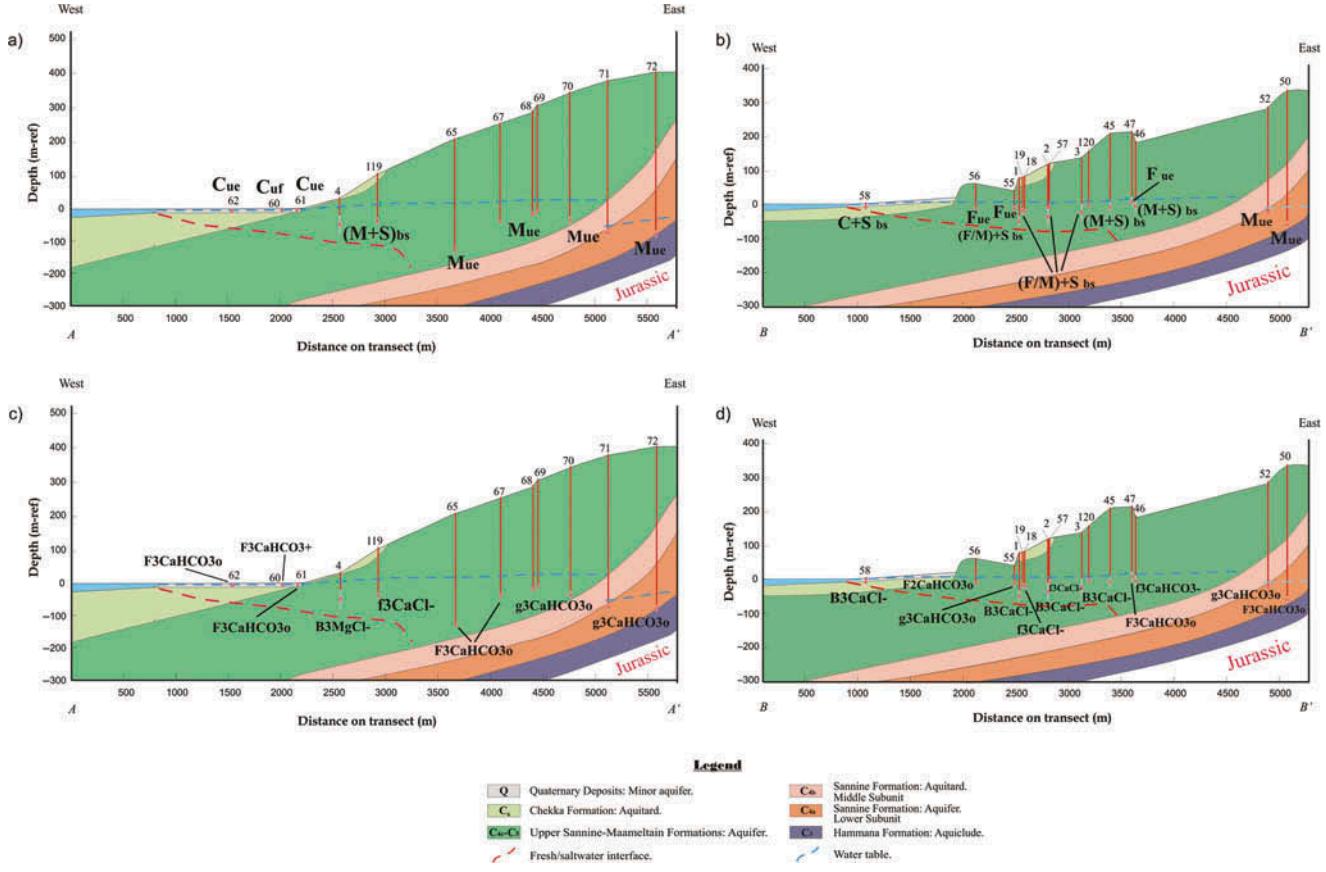

Fig. 5 Hydrogeological cross-sections east–west through Baawarta village ((a) and (c)) and Mechref village ((b) and (d)) showing the spatial distribution of hydrosomes ((a) and (b)) and the water type at depth ((c) and (d)). Codes are explained in Tables 3, 4 and 5. The freshwater–saltwater interface (≈300 mg Cl/L) is based on a geophysical survey in the mid-1960s (Geofizika 1965), and updated using the Glover solution (Cooper 1964, Charmonman 1965).

of sufficient Fe(II) and O_2 or NO_3. This does not translate into little mixing, but in the lack of reduced aquifer compartments. The relative uniformity in redox and pH justified the exclusion of redox level and pH classes as mappable facies parameters, i.e. it was redundant to give any designation since all samples were (sub)oxic and calcareous. However, the pollution index WAPI and base exchange index, BEX, showed enough variation for mapping two other groundwater qualifiers: pollution and salinization. WAPI was distributed as follows: 30% unpolluted, 52% slightly polluted and 18% moderately polluted. BEX showed 3% positive, 23% neutral and 74% negative. The spatial distribution of hydrosomes and their facies is shown in planar view in Fig. 3 and in two cross-sections in Fig. 5.

3.1.1 Mountainous limestone water (M) This hydrosome is characterized by the best water quality, showing lowest concentrations of Na, Cl, Br, SO_4, NO_3, K and many trace elements. It shows relatively high HCO_3 and Mg contents, reflecting contact with dolomitic limestone. It occurs in the eastern part of the study area more than 2500 m away from the shoreline, where it is recharged by precipitation feeding the dolomitic limestone aquifers C_{4c}–C_5 (phreatic) and C_{4a} (semi-confined). Water quality is best there, thanks to hardly any salt water intrusion, lower sea spray inputs, less agriculture, less population and a much thicker unsaturated zone (30–400 m). There is little difference in hydrochemistry between the phreatic and semi-confined aquifers, probably due to mixing in the wells and lack of confinement. Nevertheless few samples from the semi-confined aquifer showed slightly higher Fe, SiO_2, Li and Sr concentrations, testifying of a longer residence time and passage of the clayey, semi-confining C_{4b} layer.

The facies is in general unpolluted, leading to the code M_{ue}. The Mg-calcite saturation index is close to zero, BEX close to equilibrium, and the dominating water type is g3CaHCO$_3$o.

3.1.2 Damour river bank filtrate (F) This hydrosome is characterized by the lowest HCO_3, Ca, SiO_2, ^2H and ^{18}O concentrations, with relatively low Cl and SO_4 concentrations (<50 mg/L), and a relatively high NO_3 content (5–15 mg/L). It occurs within 200 m from the Damour River channel, within ~1.5 km from the shore where heavy pumping from aquifer C_{4c}–C_5 forced the river to infiltrate. The facies is unpolluted, and BEX is neutral, leading to the code F_{ue}. The calcite saturation index is close to zero, and the water type is F2CaHCO$_3$o.

3.1.3 Coastal plain water (C) The hydrochemical conditions of this hydrosome are variable, mainly due to high geochemical heterogeneities from one location to another and small thickness of the Quaternary deposits. It occurs close to the shoreline, within 900 m. The boundary between M and C is located where limestone hardrock is rising up from the coastal plain and not covered by Quaternary deposits.

This hydrosome is characterized by the lowest Cl:SO_4 and Cl:Br ratios, and the highest Ca:Mg ratio and SiO_2 concentration. This corresponds with calcite/aragonite domination of carbonate clastics in the Quaternary deposits (very low Mg content), the presence of highly soluble diatoms in the silty marine parts of the Quaternary deposits, and specific SO_4 and Br sources in the area. The latter could consist of oxidizing pyrite or agrichemicals (SO_4) and soil disinfectants (Br from methylbromide applications). The facies is slightly polluted in some parts and varies between freshening/equilibrium conditions to salinizing. Samples having low chloride content are freshening or at equilibrium (C_{uf} or C_{ue}) whereas others having higher chloride are salinizing (C_{bs}). The chemical water type is F3CaHCO$_3$+(o) and f3CaMIX-. One sample only (#58) showed a mixed C+S hydrosome with salinizing conditions.

3.1.4 Landfill leachate (L) This presence of landfill leachate is highly probable, but its extension is uncertain due to lack of wells. One well (no. 116) could tap this hydrosome, because of its elevated concentrations of chloride (1293 mg/L), boron (372 µg/L), lead (1.9 µg/L) and zinc (1160 µg/L). This sample is plotted below the B/Cl reference line constructed for the salinized samples, which reflects higher chloride content compared to the corresponding boron. The anomalous Pb and Zn concentrations may indicate well corrosion, but the high salinity is surprising given the relative shallowness of the well, the regional depth to the fresh/salt interface, and the fact that the extracted water had high salinity since its construction.

Different origins could explain the elevated salinity, for instance deep circulations where old water is involved (Emblanch *et al.* 2005a, Yuce 2007), proximity of the well to the Naameh fault, which favours upconing, or a non-marine origin. The last possibility could indeed involve leachate from the Naameh landfill (Fig. 3) which is only 1500 m eastward. Additional wells were sampled 700 m and 40 m to the south and north, respectively, but both showed freshwater with F3CaHCO$_3$o type. However, the closest well showed raised chloride (121 mg/L) and exceptionally high zinc (2900 µg/L). In conclusion, further hydrochemical research is needed to identify the true salinity source of well no. 116, and to delineate the leachate's hydrosome. If this were to really exist, then it would reveal the violation of strict regulations that was supposed to keep this landfill safe. Over the last years, no evidence has been collected to confirm any landfill leakage to the groundwater.

3.1.5 Mixed M/S This hydrosome is characterized by moderately high HCO_3 (average of 323 mg/L) with high chloride (>1000 mg/L) and sulphate (>200 mg/L). Nitrate ranges between 2 to 14 mg/L. The facies is in general moderately polluted and salinized, leading to the code $(M/S)_{ms}$. The calcite saturation index is close to zero, and the water type is b$_3$NaCl– except for one sample having b3MgCl–, with higher Cl content and doubled Ca and Mg. It could reflect more salinization with ion exchange (Mg replacing Na), or high magnesium due to presence of dolomite in the freshwater–saltwater mixing zone.

3.1.6 Mixed M+S This hydrosome characterizes the majority of water samples in the study area. It is characterized by variable HCO_3 from 200 to 455 mg/L with chloride exceeding 300 mg/L for most samples, a value that corresponds to the freshwater–saltwater mixing zone (Kresic 2007). The few samples with <300 mg Cl/L have salinizing conditions although the recent sampling campaign was conducted in April, a month of high recharge. They are expected to become more salinized in dry periods. This agrees with time-series data available for some wells that showed a difference exceeding 100 mg Cl/L between wet and dry periods.

The facies is in general slightly to moderately polluted with a salinized facies leading to the general code $(M+S)_{b/ms}$. The dominating water type is B3CaCl– for samples in the mixing zone and F3CaHCO$_3$– for samples temporarily on the freshwater side of the interface.

3.1.7 Mixed (F/M)+S This hydrosome is characterized by a moderate HCO_3 (average of 238 mg/L) with chloride sometimes exceeding 250 mg Cl/L. It is an extension of the M+S hydrosome with river filtrate contribution. Sulphate concentration mostly exceeds 60 mg/L whereas nitrate is <10 mg/L. The facies is unpolluted to slightly polluted and salinized, leading to the code $(F/M)+S_{u/bs}$. The water type is F2CaHCO$_3$– for unpolluted samples, and B3CaCl– for the slightly polluted.

3.2 Establishing baseline hydrochemistry for discerned units

Following the procedure outlined in Section 2.4, samples with bad ionic balance, filtration bias, and well corrosion inputs were eliminated *a priori*. HCSA revealed three main hydrosomes: M, F and C, for which the Natural Background Levels (NBLs) were determined (Table 6). Mixed hydrosomes, for instance M/S and M+S, and polluted samples, as indicated by WAPI, were also discarded. By putting an upper limit of NO_3 at 13 mg/L one other sample of the filtered population had to be removed.

Historical data (1979–2011) for the M hydrosome showed a significant increase in most parameters. Ca, Mg and SO_4 were doubled, Cl and Na increased by 2–5 times, whereas NO_3 recorded negligible changes. The minimum values detected in 1979 (prior to excessive pumping) for the major elements were as follows (mg/L): Na (31.4), K (1.5), Ca (64), Mg (28.8), Cl (63.8), SO_4 (27.1), HCO_3 (256) and NO_3 (5). However, this sample was classified as having a salinized facies, and hence could only be used as an upper boundary for the M hydrosome NBLs. Hierarchical clustering analysis (using Ward's method for clustering, and squared Euclidean Distance for distance calculation or similarity measure) of the M hydrosome showed two distinctive clusters, of which the higher salinity cluster was discarded. Clustering was needed because a salinized facies is inherently biased and hence cannot be indicative of natural conditions. The upper 10% of the frequency distribution of the least salinized cluster was also eliminated, and the median for the remaining 90% was taken as its representative chemistry. However, some fine tuning of Ca was required, by taking the historical value. For the F and C hydrosomes, no historical data was available, and hence after applying steps 1 to 3 of the proposed methodology, statistical analysis rendered NBL determination possible by taking the median of the 90% values as representative of NBLs.

The established NBLs for hydrosomes M, F and C were checked for their IB and SI_{MIN}, and the latter necessitated a minor adjustment of pH. The C hydrosome required further fine tuning by choosing the minimum values for trace elements. This way, the Natural Background Composition (NBCs) produced for the three hydrosomes showed a calcareous, oxic, unpolluted facies, freshening for the C hydrosome while at equilibrium for the M and F.

3.3 Salinization sources

3.3.1 Sea spray and evapo(transpi)ration The fresh end members receive marine inputs via atmospheric deposition of sea spray, which normally shows an inland decrease. The flux weighted average chloride concentration recorded in bulk precipitation (Cl_P) in the study area during the wet winter season of 2011/12 was 12.9 mg/L at 1 km from the sea shore, and 9.5 mg/L at 3.7 km. This winter had a gross precipitation only 20% higher than the average for the last 30 years while wind speeds and wind directions closely approached the normal values for 9 years (Hassan 2011). The above mentioned concentrations should therefore approach long-term average values.

Sea spray had a significant impact on rainfall composition. On average, it contributed to about 21% of SO_4, 27% of Sr, 33% of Rb and B, 73% of Li, 77% of Cl, 97% of Mg and 100% of Na, K and Br whereas for Ca and Mo the contribution was <3%. These values were derived by taking:

$$\%X_M = 100\alpha_X \, Cl_P/X_P \tag{7}$$

where $\%X_M$ is the marine contribution of constituent X (%), X_P is the concentration of X in the rainfall sample (mg/L), Cl_P is the chloride concentration in the rainfall sample (mg/L), and α_X is (X/Cl) in Mediterranean seawater (mg/L basis).

In this approach, it is assumed that: (a) fractionation of the constituents of seawater during spray formation can be ignored, and (b) there are no significant Cl sources other than the sea (Duce and Hoffman 1976, Stuyfzand 1993). The relationships of different

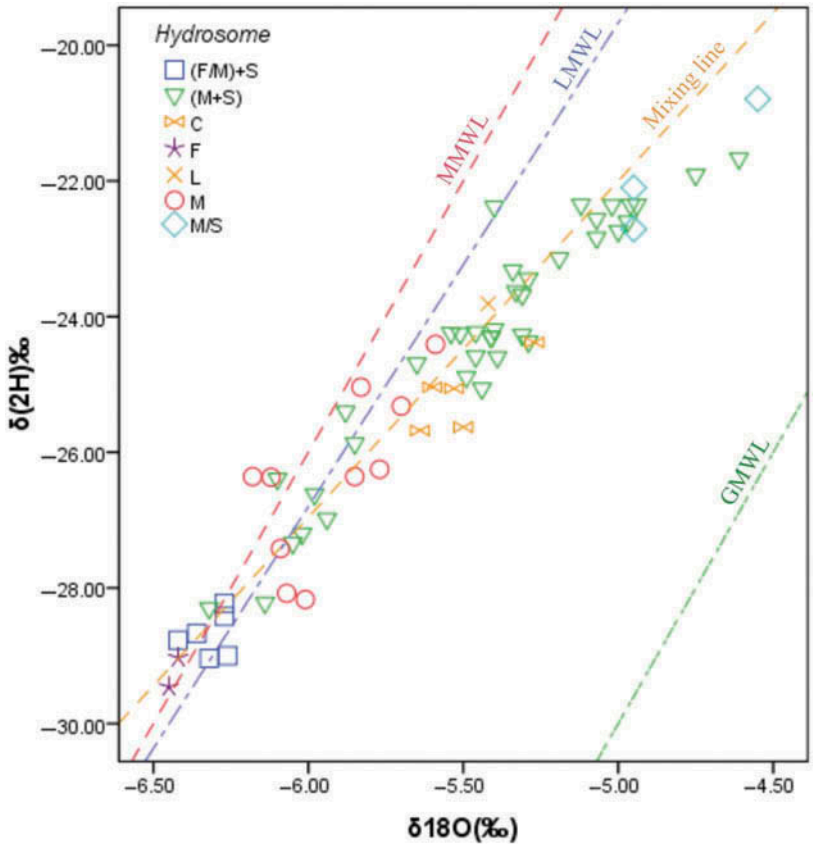

Fig. 6 δD *vs* $\delta^{18}O$ values of groundwater samples in the study area. They are compared to the Global Meteoric Water Line (GMWL, Craig 1961), the Mediterranean Meteoric Water Line (MMWL, Gat and Carmi 1970), and the Lebanese Meteoric Water Line (LMWL, Saad *et al.* 2005). The seawater–freshwater mixing line is also shown (dashed/orange).

elements with Cl were not linear because of ion-exchange (Na, K, Ca, Mg, B, Li, Mo, Rb, Sr) and dissolution/precipitation reactions (Ca, Mg, and Sr).

Evapo(transpi)ration further raised the concentrations of all constituents of bulk precipitation. Open water evaporation did not contribute much, as can be deduced from the ^{2}H–^{18}O plot in Fig. 6, showing that most groundwater samples plotted on either the mixing line with Mediterranean seawater or the Lebanese meteoric water line. The evapo-concentration factor (F) was derived by comparing the mean chloride content of baseline groundwater (Cl_{BG}) with the flux weighted mean concentration expected in rain water (Cl_P) multiplied by a factor (I) to account for the higher interception of aerosols by vegetation compared to a bulk rainfall collector (Stuyfzand 1993):

$$F = Cl_{BG}/(ICl_P) \quad (8)$$

In coastal areas, the value of I is 1.1 for surfaces with vegetation up to 0.1 m high, about 2 for dense, tall shrubs and the interior parts of forests, and 3 for the seawind facing borders of forests (Stuyfzand 1993). This yields for coastal plain water, with Cl_{BG} = 82.1 mg/L (Table 6), I = 2 and Cl_P = 12.9 mg/L, an evapo-concentration factor (F) of 3.2, which translates into 69% evapotranspiration. For the mountainous region we obtain, with Cl_{BG} = 24.1 mg/L (Table 6), I = 1.1 and Cl_P = 9.5 mg/L, a value of F = 2.3 and 56% evapotranspiration.

3.3.2 Saltwater intrusion The main source of salinization that created most of the chemical differences in the study area is saltwater intrusion. It raised the concentration of many dissolved constituents and contributed to the origin of the M/S, (M+S) and (F/M)+S hydrosomes. This was confirmed by an average Cl/Br ratio of 255 (mg/L basis), which matched saline groundwater ratio (Cartwright *et al.* 2006) and the Mediterranean sea ratio (249).

Cumulative frequency plots of the freshwaters of M and F hydrosomes and the salinized samples of the M+S, M/S, (F/M)+S hydrosomes show the extent of

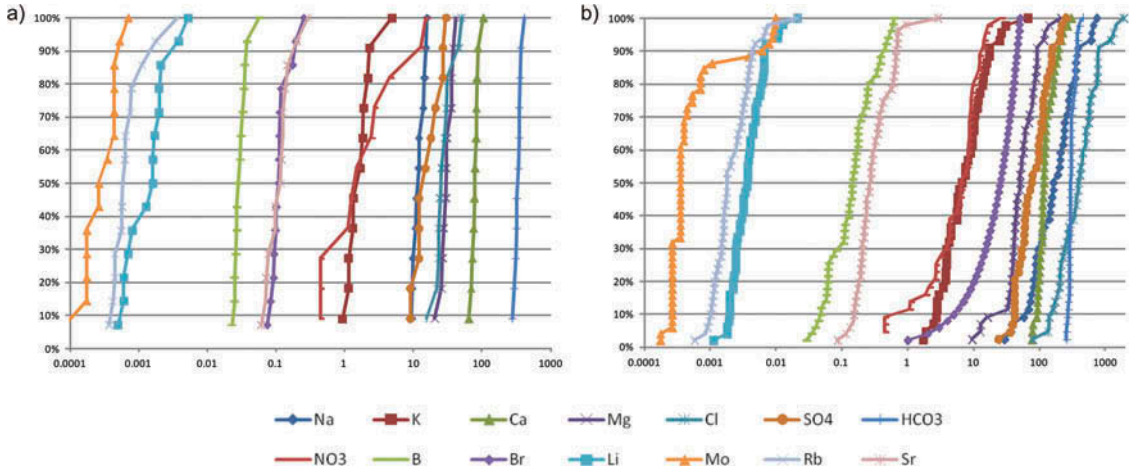

Fig. 7 Cumulative frequency (log–probability) plots for selected major elements in the freshwaters of (a) the M and F hydrosomes and (b) the salinized samples of the M+S, M/S, (F/M)+S hydrosomes.

shift from pristine conditions (Fig. 7). Concentrations of Ca, Mg, Na and K show a significant increase in salinized hydrosomes with one order of magnitude. This is due to saltwater intrusion and cation exchange associated with salinizing processes. In contrast, fresh waters show limited variation for these ions consistent with their baseline concentrations. Distributions of Cl and Br display a clear positive skew with two orders of magnitude, due to stronger salinization at high abstraction spots and closer to the shore. Also, SO_4 shows one order of magnitude increase in salinized samples. This matches with intruding saline water, since lithogenic sources such as gypsum are lacking. Anthropogenic sources may also contribute to a fraction of this variation. Variations in B, Sr, Li, Rb and Mo do not exceed one order of magnitude. Note that the shape of Na, Mg, K, Sr, B, Li and Rb curves closely follows that of chloride, which confirms a similar salinity origin. In contrast, Ca and HCO_3 show a different shape controlled by carbonate dissolution. The shapes of NO_3 and Mo are also different, probably reflecting anthropogenic inputs.

3.4 Anthropogenic inputs

WAPI was used as a preliminary index for identifying polluted samples, and then confirmed by higher than baseline concentrations. However, HCSA showed that most samples are of mixed origin with saltwater contribution (M+S and M/S); hence, the count on anthropogenic impact was exclusively given to relevant tracers with low or no contribution to Cl. Few wells showed nitrate values >13 mg/L, a threshold indicating human impact (Babiker *et al.* 2004), since the surrounding wells had low nitrate values. Bivariate plots and correlation matrices of NO_3 against EC, Cl, Ca and Mg showed no correlation except for a few samples that showed Cl enrichment supported by a positive Cl–NO_3 relationship. This reveals the existence of limited agricultural inputs from fertilizers and/or manure. These spots spread in the vicinity of agricultural fields surrounding the Damour River, in the eastern part of Haret El Naameh, in the valley of Baal El Naameh, and in the north of Dawha. According to isotopic signatures most of the samples did not show a combined increase of nitrate and $\delta^{18}O$, and Cl *versus* $\delta^{18}O$ (corrected for seawater) did not show significant variation. These observations testify that agricultural return flow was negligible.

Moreover, the same spots in Naameh and Dawha villages recorded phosphorous concentration close to or above 0.1 mg/L, suggesting contributions by sewage effluent. Hierarchical agglomerative clustering analysis of molybdenum and uranium revealed a distinctive cluster overlapping with the same spots in Naameh, and suggesting imprints of urbanization. Mo also combined with Ni disclosing a possible stainless steel interaction. In contrast, vanadium as one possible indicator of industrial origin (Moskalyk and Alfanti 2003, Wright and Belitz 2010), showed no distinctive clusters. This matched with the limited industrial activity in the area that seems to have no impact on groundwater as yet.

Consequently, anthropogenic impacts other than saltwater intrusion are still at an early stage in a few spots only. Sewage effluents and agricultural processes constitute the two major sources. It is worth noting that cesspits were widely used for sewage

disposal in the study area, but since 2011 a central system is in service that dumps its wastes, after local treatment, outside the studied aquifer. This should reduce the chances of future contamination. However, Dawha is not covered yet, which justifies an anticipated higher anthropogenic input.

4 DISCUSSION

4.1 Spatial patterns

Three spatial patterns of the studied aquifer are outlined here: (1) the distribution of salinization, (2) the downgradient evolutionary trends, and (3) the altitude of recharge zones.

4.1.1 Salinization pattern The highest salinities in the study area were recorded in Dawha and its vicinity where the $(M/S)_{ms}$ and $(M+S)_{ms}$ hydrosomes dominate (Fig. 3). This spot has low groundwater abstraction which is less than one tenth of the central zone (Damour, Naameh and Haret El Naameh), nevertheless, its enhanced salinity is explained by the direct exposure of the main aquifer (C_{4c}–C_5) to the Mediterranean Sea contrary to the central zone protected by the Chekka Formation (C_6) (Fig. 1), acting as a partial barrier for saltwater intrusion. The central zone revealed a consistent salinity pattern as going seaward, an exception occurred in parts of Mechref village where the Damour River filtrate played an adjusting role to salinity. Going further south to Delhamiye, saltwater has not significantly advanced yet since low urbanization and very few private wells with low consumption characterize this spot.

4.1.2 Evolutionary trends In calcareous porous media, it is expected that groundwater becomes more reduced and less polluted as it flows from recharge to discharge areas due to elimination of dissolved constituents like oxygen, sulphate, nitrate and heavy metals (Stuyfzand 1999, Edmunds and Shand 2008). However, this pattern does not apply to the Mountainous limestone hydrosome (M) or the slightly mixed M+S hydrosome, both of which show little hydrochemical differentiation with either depth or distance downgradient. This is explained by: (a) fissure flow in a relatively thick unsaturated zone, (b) a relatively shallow depth below the groundwater table from which the majority of wells tap groundwater, (c) little if any contact with aquitards, (d) consequently short residence times for elimination processes to become important, (e) in-well mixing, and (f) reduced downward flow connected to overexploitation.

This lack of evolutionary trends is confirmed by a rather stable strontium maturity index (SMI). The index is defined as follows:

$$\mathrm{SMI} = (\mathrm{Sr_M} - \mathrm{Sr_0})/\mathrm{Sr_0})/((\mathrm{Ca_M} + \mathrm{Mg_M} - \mathrm{Ca_0} - \mathrm{Mg_0})/(\mathrm{Ca_0} + \mathrm{Mg_0})) \quad (9)$$

where X_M is the measured concentration of X corrected for seawater contribution (meq/L), X_0 is the minimum concentration of X in the hydrosome (at a starting point of flow close to the groundwater table), corrected for seawater contribution (meq/L).

Evolutionary trends downgradient would be reflected in SMI increasing in a downgradient direction because strontium (Sr^{2+}) in carbonate rocks forms with initial formation and not from consecutive precipitation processes occurring later, i.e. it does not form in re-precipitated calcite. Therefore, a comparison of Sr^{2+} to (Ca^{2+}+Mg^{2+}) contents is a useful tool to groundwater maturity from which relative dating, residence time or flow direction can be also inferred (Emblanch *et al.* 2005b, Tulipano *et al.* 1990). In this study, the saturation index calculated for gypsum showed a negative value for all samples confirming no existence of gypsum minerals to disturb the Ca:Sr ratio.

4.1.3 Recharge zones Altitudes of recharge areas were revealed by $\delta^{18}O$, which testifies to the existence of localized recharge. A bivariate plot of land surface altitude *versus* $\delta^{18}O$ corrected for seawater contribution shows that most wells were recharged from altitudes between 100 and 400 m, which is the area of aquifer exposure to surface (Fig. 8). This estimate of altitude effect is based on an average $\delta^{18}O$ depletion of 0.28‰ per 100 m, and –4.8‰ as an initial value at sea level, which were both derived from several stations spread in Lebanon (Saad *et al.* 2005). Accordingly, no input from higher eastern mountains outside the study area existed. The broad range of $\delta^{18}O$ for the M+S hydrosome with relatively depleted values recorded in low altitude wells (–6.1‰ ± 0.1) supports the conclusion that water infiltrated at about 400 m, and then made its trip downgradient. This result matches the hydrogeology of the system (Figs 1 and 2), where the steeply inclined Hammana Formation (C_3) acts as a barrier for outside lateral groundwater flow.

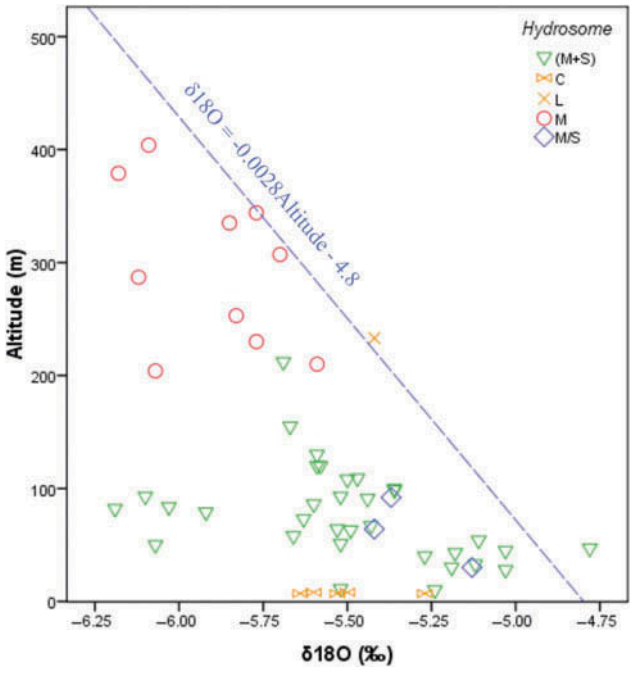

Fig. 8 Land surface altitude (m) *vs* $\delta^{18}O$ (‰) corrected for seawater contribution for recent groundwater samples collected in the study area. Samples are grouped according to hydrosome.

Razlog Aquifer in Bulgaria (BUL), the Chalk Aquifer in Denmark (DN), the Devonian Aquifer in Estonia (ES), and the Wessex Basin in the UK (UK).

The Damour aquifer showed an intermediate position with respect to most dissolved constituents compared to the four EU reference aquifers. Its most elevated Mg and lowest Sr concentration are remarkable, probably due to the dolomitic character of the Mg bearing limestone. In addition, its groundwater had the lowest concentrations of K, Fe, Mn, As, Ba, Mo and Sc.

Denmark showed the highest concentrations of Cl, Na, SO_4, Br, Mo, Fe, Mn, SiO_2 and Sc. This may reflect higher sea spray inputs, more anoxic conditions and more contact with Si-minerals in overburden or in marley beds. Estonia displayed the lowest Cl, Na and Zn concentrations, and highest levels of HCO_3, K, Ba, Li, Mn and Rb. Bulgaria showed the highest NO_3, Cr and U concentrations, and UK the highest Cu levels. These differences are hard to interpret and may be even biased due to different methods of selecting water samples that reflect baseline conditions.

4.2 Comparison with natural backgrounds elsewhere

The current groundwater quality status of the Damour Aquifer was compared with four European reference aquifers having similar limestone lithology and/or dominant hydrochemical processes, notably carbonate dissolution and saline mixing (Edmunds and Shand 2008) (Fig. 9). These included: the

4.3 Future outlook on salinization

It is evident that the studied hydrological system is facing salinization although still at a relatively early stage. Water authorities are trying to control groundwater discharge by banning the drilling of new wells, but without putting restrictions on the amount of groundwater extracted from currently running wells. Consequently, the future of this aquifer does not

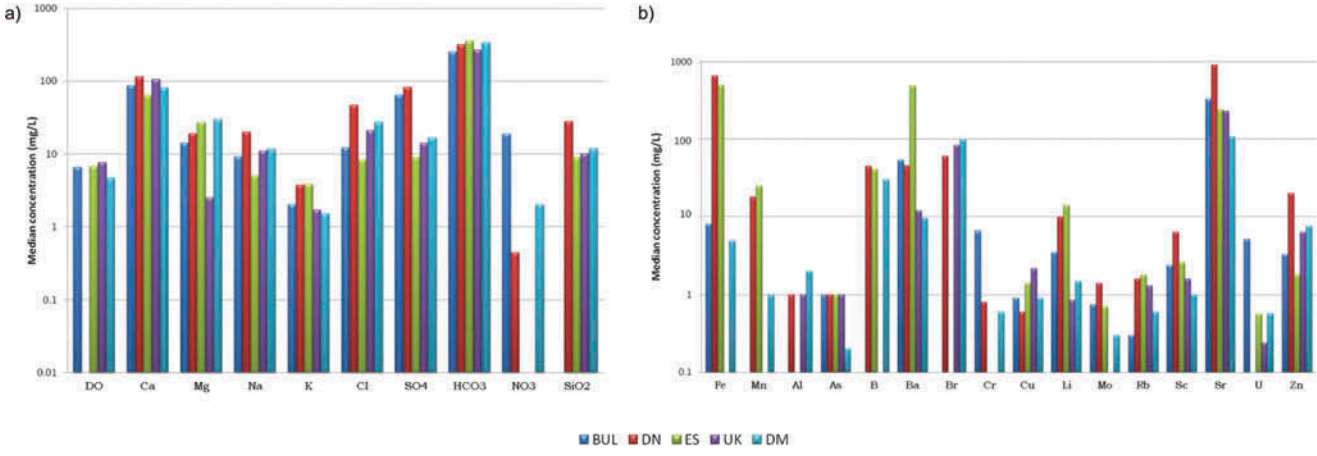

Fig. 9 Bar plots of (a) major chemical constituents and (b) main trace elements of groundwater in the M (DM) hydrosome of the Damour aquifer and four other European reference aquifers in Bulgaria (BUL), Denmark (DN), Estonia (ES), and UK (UK).

seem bright, unless optimized management strategies are pursued.

In addition, climatic factors will likely stress the system on the long-term, resulting in groundwater recharge reduction, water level decline and sea-level rise. The temperature and precipitation values predicted for West Asia by the Intergovernmental Panel on Climate Change (IPCC) show warmer conditions with lower precipitation in the next 100 years (Cruz *et al.* 2007). This will reduce groundwater recharge, and thereby add to the impact of urbanization and land use change. The global average sea-level rise estimated (for different emission scenarios) is about 34 cm (IPCC 2007), which will enhance salinization processes and enlarge the freshwater–saltwater mixing zone.

5 CONCLUSIONS

Hydrochemical System Analysis (HCSA) of the Damour aquifer system revealed the spatial distribution of groundwater bodies (hydrosomes) and hydrochemical zones (facies) within them. Concentration gradients might occur even in the same facies generating significant spatial trends, however, they were ignored here due to lack of relevant information. The following hydrosomes were identified and shown on a hydrochemical map: (1) Mountainous limestone water, (2) shallow coastal plain water, (3) Damour River bank-filtrate, and (4) mixed hydrosomes composed of freshwater from the limestone mountains, fresh river bank-filtrate and intruded saltwater of the Mediterranean Sea. This discrimination facilitated an easier hydrochemical analysis of the system, including salinization sources, anthropogenic inputs and evolutionary trends, by filtering relevant samples to be included in intended applications.

It is hypothesized that no recharge contribution exists via lateral groundwater flows from inland higher mountains, contrary to what was previously thought by others. In addition, the lack of typical downgradient hydrochemical patterns (in oxidants, pollutants and strontium maturity index) confirms the local origin of recharge to the system. This fact stresses the importance to keep current urbanization limited (≈12%), and to refrain from intensification of agriculture, which would significantly affect groundwater potentials

The baseline groundwater quality as established for the above mentioned three unmixed hydrosomes is typical for a coastal dolomitic limestone aquifer showing fresh, (sub)oxic $CaHCO_3$ water without base exchange due to fresh or salt water intrusion. After dropping salinized and polluted facies in determining NBCs, no diversity was revealed in hydrochemical facies, and hence the determined baseline was the same at both the hydrosome and facies levels. Most dissolved constituents have an intermediate position compared to four European Union reference aquifers. Closer to the shoreline, saltwater intrusion (from the Mediterranean Sea) yields a salinized facies with mostly B3CaCl– water type. However, the fraction of seawater has not exceeded 10–20% yet, which classifies the system as being at an early stage of salinization. This can be explained by a relatively late start of excessive pumping (since 1991), high productivity of the karstic aquifer system, and the role of the Damour River in providing induced recharge to its nearby wells, especially the Mechref village. A limited anthropogenic input, mainly from urban influences and agrochemical applications, also affects the system, but its minor influence is overruled by the impact of saltwater intrusion.

Complexities in assessing groundwater baseline conditions arise, in particular where: (a) historical data of pristine water is lacking, (b) the hydrological system under investigation is facing anthropogenic influences, or (c) groundwater bodies of different origins interfere. The 6-step procedure introduced in this paper stated clear and standardized steps to be followed in different settings. Biased samples were eliminated, and then two sieving stages, using Water Pollution Index (WAPI) and NO_3 concentrations, were enough to drop polluted samples. NO_3 was needed as another way of individual selection because WAPI takes a mean value of normalized concentrations, meaning it can have hidden elements. The frequency distribution could also eliminate the highest values; however, in our case no significant outliers appeared. In addition, HCSA defined all water bodies requiring natural concentrations precluding salinized samples, mixed redox and intermixed hydrosomes. This was a further step of subdividing the population, and it also warranted a detailed determination of natural background levels (NBLs) by revealing the appropriate diversity for each hydrosome and its subsequent facies. To date, this distinction is a unique outcome of HydroChemical System Analysis incorporation. It is noteworthy that NBLs for trace elements below detection limit (e.g. Fe, As, Ge, La and Sb) might be criticized against accuracy, however, this does not harm the proposed methodology. Such discrepancy arises from the

precision of the analytical tests, which are improved over time toward better detection.

Acknowledgements We would like to thank all citizens who were cooperative with the sampling campaign. Special thanks goes to the municipalities of Mechref, Naameh, Baawerta and Damour for providing all needed support. We are also grateful for Beirut Water Authority which made all government wells in the study area accessible. The constructive comments of reviewer Kristine Walraevens and an anonymous reviewer contributed to some essential improvements of the manuscript.

REFERENCES

Abdul Rahman, A.C., 2007. Environmental isotopic and hydrochemical study of water in the karst aquifer and submarine springs of the Syrian coast. *Hydrogeology Journal*, 15, 351–364.

Ajam, N. and Saa'd, H., 1980a. *Technical report on four drilled wells in Damour area, Lebanon*. Beirut: Ministry of Water and Electric Resources.

Ajam, N. and Saa'd, H., 1980b. *Technical report on six drilled wells in Haret en Naame-Mechrif area, Lebanon*. Beirut: Ministry of Water and Electric Resources.

Alcalá, F. and Custodio, E., 2004. Use of the Cl/Br ratio as tracer to identify the origin of salinity in some Spanish coastal aquifers. *In*: *18th salt water intrusion meeting*, *Cartagena, Spain*.

Arkadan, A., 1999. *The geology, geomorphology and hydrogeology of the Damour-Awali area coastal and hinterland*. MS Thesis. American University of Beirut, Beirut, Lebanon.

Arkadan, A. 2008. Climatic changes in Lebanon, predicting uncertain precipitation events—Do climatic cycles exist? *In*: F. Zereini and H. Hötzl, eds. *Climatic changes and water resources in the Middle East and North Africa*. Berlin: Springer, Environmental Science and Engineering, 59–74.

Babiker, I., *et al*., 2004. Assessment of groundwater contamination by nitrate leaching from intensive vegetable cultivation using geographical information system. *Environment International*, 29, 1009–1017.

Bobba, A.G., 2007. Groundwater development and management of coastal aquifers (including island aquifers) through monitoring and modeling approaches. *In*: M. Thangarajan, ed. *Groundwater resource evaluation, augmentation, contamination, restoration, modeling and management*. New Delhi: Springer, 283–333.

Bouchaou, L., *et al*., 2008. Application of multiple isotopic and geochemical tracers for investigation of recharge, salinization, and residence time of water in the Souss-Massa aquifer, southwest of Morocco. *Journal of Hydrology*, 352, 267–287.

Brenot, A., *et al*., 2008. Interaction between different water bodies in a small catchment in the Paris basin (Brévilles, France): tracing of multiple Sr sources through Sr isotopes coupled with Mg/Sr and Ca/Sr ratios. *Applied Geochemistry*, 23, 58–75.

CAMP, 2004. *Coastal Area Management Programme (CAMP) Lebanon*. Beirut: UNEP, National Project of the Mediterranean Action Plan (MAP) of UNEP, 253.

Camp, M.V. and Walraevens, K., 2008. Identifying and interpreting baseline trends. *In*: W.M. Edmunds and P. Shand, eds. *Natural groundwater quality*. Oxford: Blackwell Publishing Ltd, 131–154.

Cartwright, I., *et al*., 2006. Cl/Br ratios and environmental isotopes as indicators of recharge variability and groundwater flow: an example from the southeast Murray Basin, Australia. *Chemical Geology*, 231, 38–56.

Charmonman, S., 1965. A solution of the pattern of fresh-water flow in an unconfined coastal aquifer. *Journal of Geophysical Research*, 70, 2813–2819.

Cooper, H.H., 1964. *Sea water in the coastal aquifers*. Washington, DC: U Geological Survey Water-Supply Paper 1613-C, 84.

Craig, H., 1961. Isotopic variations in meteoric waters. *Science*, 133, 1702–1708.

Cruz, R.V., *et al*., 2007. *Asia. Climate change 2007: impacts, adaptation and vulnerability*. Contribution of Working Group II to the fourth assessment report of the Intergovernmental Panel on Climate Change. M.L. Parry, *et al*., eds. *An assessment of the Intergovernmental Panel on Climate Change*. Cambridge: Cambridge University Press, 469–506.

Dar Al-Handasah, 1999. *Beirut southern suburbs rehabilitation Lot VIII-Doha Aramoun Damour water wells, progress report*. Beirut: Council for Development and Reconstruction (CDR), 125.

de Montety, V., *et al*., 2008. Origin of groundwater salinity and hydrogeochemical processes in a confined coastal aquifer: case of the Rhône delta (Southern France). *Applied Geochemistry*, 23, 2337–2349.

Duce, R.A. and Hoffman, E.J., 1976. Chemical fractionation at the air/sea interface. *Annual Review of Earth Planetary Sciences*, 4, 187–228.

Edmunds, W.M., *et al*., 2003. The natural (baseline) quality of groundwater: a UK pilot study. *Science of the Total Environment*, 310, 25–35.

Edmunds, W.M. and Shand, P., 2008. Groundwater baseline quality, *In*: W.M. Edmunds and P. Shand, eds. *Natural groundwater quality*. Blackwell Publishing Ltd, 1–21.

El-Fiky, A., 2010. Hydrogeochemical characteristics and evolution of groundwater at the Ras Sudr-Abu Zenima area, Southwest Sinai, Egypt. *Earth Science*, 21(1),79–109.

El-Hakim, M. and Bakalowicz, M., 2007. Significance and origin of very large regulating power of some karst aquifers in the Middle East. Implication on karst aquifer classification. *Journal of Hydrology*, 333, 329–339.

Emblanch, C., *et al*., 2005a. Environmental tracing methods. *In*: Tulipano, *et al*., eds. *Groundwater management of coastal karstic aquifers*. Luxemburg: COST Action 621, Final Report, EUR 21366, COST Office, 363.

Emblanch, C., *et al*., 2005b. Environmental tracing for outlining fresh groundwater flow in a coastal karstic aquifer. *In*: Tulipano, *et al*., eds. *Groundwater management of coastal karstic aquifers*. Luxemburg: COST Action 621, Final Report, EUR 21366, COST Office, 363.

Essink, G., 2001. Improving fresh groundwater supply-problems and solutions. *Ocean and Coastal Management*, 44, 429–449.

Gat, J.R. and Carmi, I., 1970. Evolution of the isotopic composition of atmospheric waters in the Mediterranean Sea area. *Journal of Geophysical Research*, 75, 3039–304.

Geophyzika, 1965. *Report on geophysical investigations in the southern coastal zone*. Zagreb: Geophyzika Enterprise for Applied Geophysics.

Hassan, G., 2011. *The national wind atlas of Lebanon*. Beirut: UNDP-CEDRO project, 63 p.

IPCC (Intergovernmental Panel on Climate Change), 2007. *Contribution of Working Groups I, II and III to the fourth assessment report of the Intergovernmental Panel on Climate Change*. Geneva: IPCC, 104.

Kafri, U. and Arad, A., 1979. Current subsurface intrusion of Mediterranean seawater—a possible source of groundwater salinity in the Rift Valley system, Israel. *Journal of Hydrology*, 44, 267–287.

Kempe, S., *et al*., 2006. Al-Daher Cave (Bergish), Jordan, the first extensive Jordanian limestone cave: a convective Carlsbad-type cave? *Journal of Cave and Karst Studies*, 68 (3), 107–114.

Khadra, W.M., 2003. Hydrogeology of the Damour-Upper Sannine-Maameltain Aquifer. MS Thesis. American University of Beirut, Beirut, Lebanon.

Korfali, S. and Jurdi, M., 2007. Assessment of domestic water quality: case study, Beirut, Lebanon. *Environmental Monitoring and Assessment*, 135, 241–251.

Korfali, S. and Jurdi, M., 2009. Provision of safe domestic water for the promotion and protection of public health: a case study of the city of Beirut, Lebanon. *Environmental Geochemical Health*, 31, 283–295.

Kresic, N., 2007. *Hydrogeology and groundwater modeling*. 2nd ed. New York: CRC Press, 807.

Lebanese Ministry of Environment, 2001. *Lebanon State of the Environment Report*. Beirut: ECODIT/LEDO, 246.

Lee, J.Y. and Song, S.H., 2007. Groundwater chemistry and ionic ratios in a western coastal aquifer of Buan, Korea: implication for seawater intrusion. *Geosciences Journal*, 11(3), 259–270.

Mandel, S., *et al*., 1972. Groundwater flow in calcareous aquifers in the vicinity of Barcelona, Spain. *Bulletin of International Association of Hydrological Sciences*, 17, 77–83.

Mendizabal, I. and Stuyfzand, P.J., 2009. Guidelines for interpreting hydrochemical patterns in data from public supply well fields and their value for natural background groundwater quality determination. *Journal of Hydrology*, 379, 151–163.

Meteorological Service, 2010. Meteorological *Data Archive, Lebanon Weather, 1985-2010*. Unpublished weather reports from Beirut International Airport weather station. Beirut: General Directorate of Civil Aviation.

Morse, J.W. and Mackenzie, F.T., 1990. Geochemistry of Sedimentary Carbonates, Elsevier, 707.

Moskalyk, R.R. and Alfanti, A.M., 2003. Processing of vanadium: a review. *Mineral Engineering*, 16, 793–805.

Petelet-Giraud, E., *et al*., 2007. Geochemical and isotopic constraints on groundwater-surface water interactions in a highly anthropized site. The Wolfen/Bitterfeld megasite (Mulde subcatchment, Germany). *Environmental Pollution*, 148, 707–717.

Post, V.E., 2005. Fresh and saline groundwater interaction in coastal aquifers: is our technology ready for the problems ahead? *Hydrogeology Journal*, 13, 120–123.

Saad, Z., *et al*., 2004. Chemical and isotopic composition of water from springs and wells in the Damour River Basin and the Coastal Plain in Lebanon. *Journal of Environmental Hydrology*, 12, 1–13.

Saad, Z., *et al*., 2005. Chemical and isotopic composition of rainwater in coastal and highland regions in Lebanon. *Journal of Environmental Hydrology*, 13, 1–11.

Saadeh, M., 2008. *Influence of overexploitation and seawater intrusion on the quality of groundwater in Greater Beirut*. Thesis (PhD). Aachen University, Germany.

Sanford, W.E. and Pope, J.P., 2010. Current challenges using models to forecast seawater intrusion: lessons from the Eastern Shore of Virginia, USA. *Hydrogeology Journal*, 18, 73–93.

Stigter, T.Y., *et al*., 1998. A hydrogeological and hydrochemical explanation of the groundwater composition under irrigated land in a Mediterranean environment, Algarve, Portugal. *Journal of Hydrology*, 208, 262–279.

Stuyfzand, P.J., 1984. Groundwater quality evolution in the upper aquifer of the coastal dune area of the western Netherlands. *In*: E. Eriksson, ed., *Hydrochemical balances of freshwater systems, Proceedings of Uppsala Symposium*. Wallingford: International Association of Hydrological Sciences, IAHS Publ. 150, 87–98. http://iahs.info/uploads/dms/150009.pdf [Accessed 29 August 2014].

Stuyfzand, P.J., 1986. A new hydrochemical classification of water types: principles and application to the coastal dunes aquifers system of the Netherlands. *In*: *Proceedings of 9th salt water intrusion meeting*. Delft: Delft University of Technology, 641–655.

Stuyfzand, P.J., 1987. Influences of filtration and storage of groundwater samples on sample composition. *Trends in Analytical Chemistry (TrAC)*, 6, 50–54.

Stuyfzand, P.J., 1989. A new hydrochemical classification of water types. *In*: S. Ragone, ed., *Regional characterization of water quality, Proceedings of Baltimore Symposium*. Wallingford: International Association of Hydrological Sciences: IAHS Publ. 182, 89–98. http://iahs.info/uploads/dms/iahs_182_0089.pdf [Accessed 29 August 2014].

Stuyfzand, P.J., 1993. *Hydrochemistry and hydrology of the coastal dune area of the Western Netherlands*. Thesis (PhD). Vrije Univ Amsterdam, KIWA, 366.

Stuyfzand, P.J., 1999. Patterns in groundwater chemistry resulting from groundwater flow. *Hydrogeology Journal*, 7, 15–27.

Stuyfzand, P.J., 2005. Mapping groundwater bodies with artificial or induced recharge, by determination of their origin and chemical facies. *In*: *Proceedings of 5th International symposium on management of aquifer recharge*. Berlin: ISMAR-5, 839–850.

Stuyfzand, P.J., 2008. Base exchange indices as indicators of salinization or freshening of (Coastal). *In*: *Proceedings of 20th saltwater intrusion meeting*. Naples, FL: SWIM, 262–265.

Stuyfzand, P.J., 2012. *Hydrogeochemcal (HGC 2.1), for storage, management, control, correction and interpretation of water quality data in Excel® spread sheet*. Nieuwegein: KWR report BTO 2012. 244(s), 76.

Stuyfzand, P.J. and Stuurman, R.J., 2006. Origin, distribution and chemical mass balances of non-anthropogenic, brackish and (hyper)saline groundwaters in the Netherlands. *In*: *Proceedings of 1st SWIM-SWICA joint saltwater intrusion conference*. Cagliari: SWIM-SWICA, 151–164.

Tulipano, L., *et al*., 1990. An example of multitracing approach in the studies of karstic and coastal aquifers. *In*: G. Gunay *et al*., eds. *Hydrogeological processes in Karst Terranes. Antalya symposium 1990*. Wallingford: International Association of Hydrological Sciences, IAHS Publ. 207, 381–389. http://iahs.info/uploads/dms/iahs_207_0381.pdf [Accessed 29 August 2014].

Tulipano, L., *et al*., 2005. *Groundwater management of coastal karstic aquifers*. Luxemburg: COST Action 621, Final Report, EUR 21366, COST Office, 363.

Weinstein, Y., *et al*., 2007. Submarine groundwater discharge in the southeastern Mediterranean (Israel). *Radioactivity in the Environment*, 8, 360–372.

Wright, M.T. and Belitz, K., 2010. Factors controlling the regional distribution of vanadium in groundwater. *Ground Water*, 48 (4), 515–525.

Yuce, G., 2007. A Geochemical study of the groundwater in the Misli basin and environmental implications. *Environmental Geology*, 51, 857–868.